High Levels of Hepatitis B Virus After the Onset of Disease Lead to Chronic Infection in Patients With Acute Hepatitis B

Hiroshi Yotsuyanagi,[1,a] Kiyoaki Ito,[2,5,a] Norie Yamada,[1,3,4] Hideaki Takahashi,[3] Chiaki Okuse,[3] Kiyomi Yasuda,[4] Michihiro Suzuki,[3] Kyoji Moriya,[1] Masashi Mizokami,[2] Yuzo Miyakawa,[6] and Kazuhiko Koike[1]

[1]Department of Internal Medicine, Graduate School of Medicine, University of Tokyo, Bunkyo; [2]The Research Center for Hepatitis and Immunology, National Center for Global Health and Medicine, Ichikawa; [3]Division of Gastroenterology and Hepatology, Department of Internal Medicine, St Marianna University School of Medicine, Kawasaki; and [4]Department of Internal Medicine, Center for Liver Diseases, Kiyokawa Hospital, Suginami, [5]Department of Microbiology and Immunology, Aichi Medical University School of Medicine, and [6]Miyakawa Memorial Research Foundation, Minato, Tokyo, Japan

Background. Some patients with acute hepatitis B virus (HBV) infection develop chronic infection. However, the method for identifying these patients has not been established.

Methods. We followed 215 Japanese patients with acute HBV infection until the clearance of hepatitis B surface antigen (HBsAg) or the development of chronic infection. Levels of HBsAg and HBV DNA were serially monitored from the onset.

Results. Of the 215 patients, 113 (52.5%) possessed HBV genotype A, 26 (12.0%) genotype B, and 73 (34.0%) genotype C. Twenty-one of the 215 (9.8%) developed chronic infection, with the persistence of HBsAg for >6 months. The rate of chronicity of genotype A, B, and C was 12.4%, 3.8%, and 8.2%. Of the 21 patients, only 6 (2.8%) patients, including 5 with genotype A, failed to clear HBsAg within 12 months. Levels of HBsAg at 12 weeks and HBV DNA at 4 weeks were useful for distinguishing the patients who became chronic from those who did not ($P < .001$ and $P < .001$, respectively). Likewise, the levels of HBsAg at 12 weeks and HBV DNA at 8 weeks were useful for discriminating between the patients who lost HBsAg within 12 months and those who did not ($P < .01$ and $P < .05$, respectively).

Conclusions. In acute HBV infection, clearance of HBV may happen between 6 and 12 months from the onset. Only those who fail to clear HBV within 12 months from the onset may develop chronic infection.

Keywords. hepatitis B virus antigen; hepatitis B virus; genotype.

The clinical outcome of acute hepatitis B is self-limited in the majority of immunocompetent adults. However, some patients run a prolonged or even chronic course, or are complicated by acute liver failure. Several factors are implicated in different clinical courses.

Hepatitis B virus (HBV) genotypes and subtypes are known to influence the clinical outcome of acute hepatitis B. For instance, HBV subgenotype B1 is associated with fulminant hepatic failure in acute hepatitis B [1]. On the other hand, genotype A is associated with chronic sequelae [2–5]. Furthermore, patients with subgenotype C2 are more likely to develop chronic infection than those with subgenotype B2 [6]. These characteristics may reflect viral kinetics in acute HBV infection that would differ among HBV infections with distinct genotypes/subgenotypes, but little is known about them.

Quantitation of hepatitis B surface antigen (HBsAg), in addition to HBV DNA, has been introduced to analysis of viral kinetics in patients with chronic hepatitis B in recent years. HBsAg levels are also useful for estimating

Received 14 February 2013; accepted 9 May 2013; electronically published 23 May 2013.

[a]H. Y. and K. I contributed equally to this work.

Correspondence: Hiroshi Yotsuyanagi, MD, Department of Internal Medicine, Graduate Institute of Medicine, University of Tokyo, 7-3-1, Hongo, Bunkyo, Tokyo 113-8655, Japan (hyotsu-tky@umin.ac.jp).

Clinical Infectious Diseases 2013;57(7):935–42

DOI: 10.1093/cid/cit348

viral loads and predicting the response to antiviral treatments [7–9], and for determining the natural history of chronic hepatitis B [10, 11]. Therefore, HBsAg and HBV DNA would be instrumental in foretelling the outcome of acute hepatitis B. However, the clinical utility of these markers in patients with acute hepatitis B is largely unknown.

Therefore, the aim of the present study was to examine differences in viral kinetics among patients with acute hepatitis B, who were infected with HBV of different genotypes, and evaluate the usefulness of quantifying HBsAg and HBV DNA for predicting the clinical outcome.

PATIENTS AND METHODS

Patients

This was a retrospective study of patients who were diagnosed with acute hepatitis B in our institutions during 1994 through 2010. Criteria for the diagnosis of acute hepatitis B were (1) acute onset of liver injury without a previous history of liver dysfunction; (2) detection of HBsAg in the serum; (3) immunoglobulin M (IgM) antibody to HBV core (anti-HBc) in high titers (detectable in serum samples diluted 10-fold) [3]; (4) absence of a past or family history of chronic HBV infection; and (5) exclusion of coinfection with hepatitis A virus, hepatitis C virus, or other hepatotropic viruses by serologic testing. Among the 232 patients who met these criteria, 215 patients (159 men and 56 women with a mean age of 31.8 ± 10.0 years) whose serum samples were available for virologic analyses were included in the study. No patient developed liver failure.

No patient received antiviral treatment. Of the 215 patients, 159 (74.0%) patients could be regularly followed up until the confirmation of clinical outcomes. Based on the duration of HBsAg (defined as the interval between the onset [defined by the first visit] and the last visit with detectable HBsAg), we classified the 159 patients into the following 4 groups (the duration of HBsAg is indicated in parentheses): group 1 (<3 months); group 2 (3–6 months); group 3 (>6–12 months); and group 4 (>12 months). Changes in virologic parameters were analyzed in relation with clinical characteristics. The study was approved by the ethics committees of our institutions, and written informed consent was obtained from each patient.

Quantification of Serologic Markers for HBV Infection and HBV DNA

HBsAg had been measured quantitatively by chemiluminescent enzyme-linked immunosorbent assay (ELISA; Sysmex JAPAN Co, Ltd, Kobe, Japan) every 2–4 weeks, until the clinical outcome was known. It has a dynamic range of 0.03–2, 500 IU/mL. Serum samples scaling out from this range were diluted so as to contain them within it. Antibody to hepatitis B s antigen (anti-HBs), hepatitis B e antigen (HBeAg), and IgM anti- HBc were determined by ELISA (Abbott JAPAN Co, Ltd, Tokyo, Japan). Levels of HBV DNA were determined using the COBAS TaqMan HBV v.2.0 kit (Roche Diagnostics, Basel, Switzerland), which has a dynamic range over 2.1–9.0 log copies/mL.

HBV Genotyping

The HBV genotype was determined by a genotype-specific probe assay (Smitest HBV genotyping Kit, Genome Science, Fukushima, Japan) as previously reported [12].

Molecular Evolutionary Analyses

HBV genotype A started to prevail in Japan merely several years ago, suggesting that it was imported to Japan only recently [3, 13]. Therefore, genomic sequences of HBV genotype A (HBV/A), recovered from sera of patients with acute HBV infection, would be closely related to one another and with those reported from abroad. To evaluate this possibility, 20 HBV/A samples were selected randomly and sequenced by the method reported previously [14].

The number of nucleotide substitutions per site was estimated by the 6-parameter method [15], and a phylogenetic tree was constructed by the neighbor-joining method [16] based on the numbers of substitutions. To confirm the credibility of phylogenetic analyses, bootstrap resampling tests were carried out 1000 times [17].

Statistical Analyses

Categorical variables were compared by χ^2 test or Fisher exact test, and continuous variables by the Mann-Whitney U test. $P < .05$ was considered statistically significant. Receiver operating characteristic (ROC) analysis was performed to compute the area under the ROC curves for viral markers to determine cutoff points for predicting the outcome.

RESULTS

Distribution of HBV Genotypes in Patients With Acute Hepatitis B

HBV genotypes were determined in 215 of the 232 (93%) patients with acute hepatitis B. Of the 215 patients, genotype A was detected in 113 (52%), B in 26 (12%), C in 73 (33%), D in 1 (1%), E in 1 (1%), and F in 1 (1%). The distribution of genotypes was compared among 4 periods during 1994 through 2010 (Table 1). The proportion of patients with genotype A gradually increased to 65.9% in 2007–2010; it was higher than those in the earlier periods (34.4% in 1994–1998 [$P = .002$], 36.8% in 1999–2002 [$P = .002$], and 51.9% in 2003–2006 [$P = .093$]).

Phylogenetic Relationship Among HBV Strains of Genotype A

We randomly selected 11 HBV/A strains sampled in 2007–2010 and 9 of those in 2001–2006, and constructed a molecular evolutionary tree (Figure 1). All 20 samples had similar nucleotide sequences with a concordance of 99%. They were close to previously

Table 1. Prevalence of Hepatitis B Virus Genotypes in Patients With Acute Hepatitis B During 4 Chronologic Periods

Period	Genotype A	Genotype B	Genotype C	Others
1994–1998 (n = 32)	11[a] (34.4%)	3 (9.3%)	18 (56.3%)	0
1994–1998 (n = 38)	14[b] (36.8%)	4 (10.5%)	20 (52.7%)	0
1994–1998 (n = 54)	28[c] (51.9%)	6 (11.1%)	19 (35.1%)	1 (1.9%)
1994–1998 (n = 91)	60[a,b,c] (65.9%)	13 (14.3%)	16 (17.6%)	2 (2.2%)
Total (N = 215)	113 (52.5%)	26 (12.0%)	73 (34.0%)	3 (1.5%)

[a] $P = .0032$.

[b] $P = .0014$.

[c] $P = .02$.

reported genotype A2 sequences from Western countries. The results support the possibility that HBV/A was imported to Japan only recently and has been spreading throughout the country.

Clinical Features Among Patients Infected With HBV of Different Genotypes

Clinical features of patients with acute hepatitis B of different genotypes are compared in Table 2. The mean age was no different among patients infected with HBV of different genotypes. The proportion of men was higher in genotype A or B than C infection (93.8% or 80.7% vs 39.7% [A vs C, $P < .001$; B vs C, $P < .001$]).

The maximum alanine aminotransferase (ALT) level was lower in patients with genotype A than in those with genotype C (2126 ± 938 vs 2857 ± 1668 IU/L, $P = .002$). The maximum bilirubin level was higher in patients with genotype A (7.1 ± 6.4 mg/dL) or C (9.0 ± 7.5 mg/dL) than in those with genotype B (4.8 ± 3.3 mg/dL) (A vs B, $P = .003$; B vs C, $P < .001$). Regarding viral markers, the peak HBV DNA level was higher in patients with genotype A than in those with genotype C (6.3 ± 1.7 vs 4.9 ± 1.5 log copies/mL, $P < .001$). HBeAg was detected in 95 of the 121 (77.3%) patients with genotype A, 24 of the 28 (88.5%) with genotype B, and 37 of the 58 (65.5%) with genotype C (A vs C, $P = .036$). Men who have sex with men were more frequently represented among patients with genotype A than B or C (31.4% vs 4.8% or 11.3% [A vs B, $P = .017$; A vs C, $P = .002$]). Antibody to human immunodeficiency virus (anti-HIV) was examined in 72 of the 113 (63.7%) patients with genotype A, 7 of the 26 (26.9%) with genotype B, 58 of the 73 (79.5%) with genotype C, and 1 with genotype E. Anti-HIV was detected in 7 of the 72 (9.7%) patients with genotype A, and the other 96 patients tested for anti-HIV showed negative results. All of the 7 patients with anti-HIV cleared HBsAg from the serum within 6 months without antiviral treatment.

Among the 215 patients whose HBV genotypes were determined, 159 could be followed until the confirmation of clinical outcomes. The distribution of HBsAg-positive period is compared among patients with different genotypes. Group 1 (HBsAg persisting for <3 months) comprised 84 patients; group 2 (3–6 months) comprised 54 patients; group 3 (>6–12 months) comprised 15 patients; and group 4 (>12 months) comprised 6 patients. HBsAg remained >6 months in 21 of the 215 (9.8%) patients, including 14 of the 113 (12.4%) with genotype A, 1 of the 26 (3.8%) with genotype B, and 6 of the 73 (8.2%) with genotype C. Among the 21 patients, 15 (71.4%) cleared HBsAg within 12 months from the onset, and were classified into group 3. The remaining 6 (5 with genotype A and 1 with genotype B) who failed to clear HBsAg within 12 months were classified into group 4. All of the 6 were negative for anti-HIV. The proportion of group 4 was 6.0% in the patients with genotype A, 4.0% in those with genotype B, and 0% in those with genotype C.

The mean duration of HBsAg was 13.9 ± 8.7 weeks in patients with genotype A, 7.1 ± 5.3 weeks in those with genotype B, and 9.6 ± 7.6 weeks in those with genotype C, presuming the duration of HBsAg in group 4 at 12 months. The duration was longer in patients with genotype A than in those with B or C (A vs B, $P < .001$; A vs C, $P = .04$).

Prediction of the Outcome by the Duration of HBsAg

Table 2 shows that the duration of HBsAg among patients with genotype A varied to a higher extent than that among those with other genotypes. Therefore, we determined HBsAg and HBV DNA levels serially, and evaluated them for the ability to predict the outcome of acute hepatitis B in patients with genotype A.

Serial changes in HBsAg levels are shown in Supplementary Figure 1*A*. HBsAg levels declined more slowly in group 2 than group 1, as well as in group 3 than group 2. In group 4, HBsAg reelevated at 12 weeks after the onset. Figure 2 compares HBsAg levels among groups 1–4 at different intervals from the onset. HBsAg at 8 weeks from the onset was useful for distinguishing group 3 or 4 from group 1 or 2. Likewise, HBsAg at 12 weeks from the onset was helpful for discriminating among groups 2, 3, and 4.

Prediction of the Outcome by HBV DNA

We also studied serial changes of HBV DNA in patients with genotype A, and examined if they also were useful for predicting the clinical outcome of acute hepatitis B. Supplementary Figure 1*B* shows serial changes in HBV DNA levels in patients in 4 groups. Although the reelevation of HBV DNA was not observed, the decline of HBV DNA was quite slow in group 4. Figure 3 compares HBV DNA levels among groups 1–4 at different intervals from the onset. HBV DNA at 4 weeks from

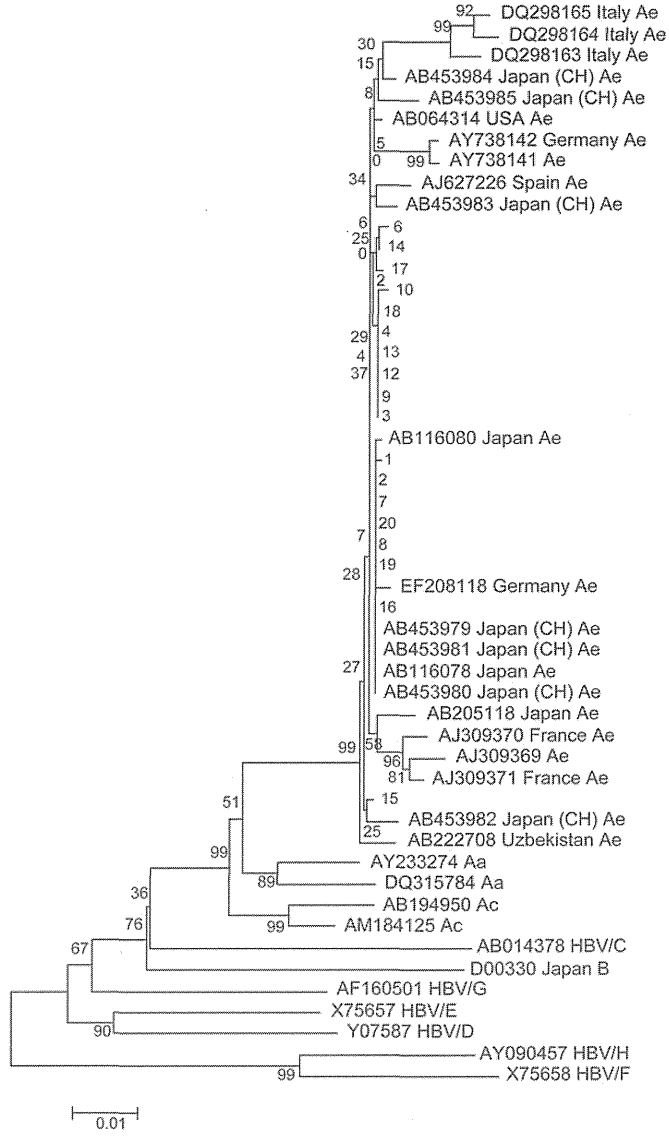

Figure 1. Evolutionary relationships of 86 hepatitis B virus genotype A taxa, including 20 from the present cases. The evolutionary history, inferred using the neighbor-joining method, shows that all 20 samples had similar nucleotide sequences close to previously reported genotype A2 sequences from Western countries.

the onset was useful for distinguishing group 3 or 4 from group 1 or 2. Likewise, HBV DNA levels at 8 weeks from the onset were useful for discriminating between group 4 and group 3, as well as for distinguishing group 3 or 4 from group 1 or 2.

Levels of HBsAg and HBV DNA for Predicting Persistent Infection

As the levels of HBsAg at 12 weeks and HBV DNA at 8 weeks from the onset were useful for distinguishing group 4 from the other groups, we evaluated the appropriate levels for predicting persistent infection in patients with genotype A. When we set the cutoff value of HBsAg at 1000 IU/mL based on the ROC analysis, both the positive predictive value and the negative predictive value were 100% with high sensitivity (100%) and specificity (98.1%). Likewise, when we set the cutoff value of HBV DNA at 10^6 log IU/mL based on the ROC analysis, both the positive predictive value and the negative predictive value were 100% with high sensitivity (100%) and specificity (96.4%). Therefore, HBsAg at 12 weeks >1000 IU/mL or HBV DNA at 8 weeks >10^6 log copies/mL is useful for predicting persistent infection.

DISCUSSION

In Japan, as shown in Table 1, the dominant HBV in acute hepatitis has been shifting from genotype C to A [3, 5, 14, 18]. The fact that nucleotide sequences of HBV/A isolates from patients

Table 2. Baseline Characteristics and the Duration of Hepatitis B Surface Antigen in Patients With Acute Hepatitis B Virus With Different Hepatitis B Virus Genotypes

	HBV Genotypes					
Features	A (n = 113)	B (n = 26)	C (n = 73)	D (n = 1)	E (n = 1)	F (n = 1)
Age, y	30.8 ± 9.5	32.3 ± 9.5	33.3 ± 10.9	27	26	58
Male	106 (93.8%)[a]	21 (80.7%)[b]	29 (39.7%)[a,b]	0	0	1 (100%)
Transmission routes Identified	102 (90.2%)	21 (80.8%)	53 (72.6%)	1 (100%)	1 (100%)	1 (100%)
Heterosexual	70 (68.6%)	19 (90.4%)	47 (88.7%)	1 (100%)	1 (100%)	1 (100%)
MSM	32 (31.4%)[c,d]	1 (4.8%)[c]	6 (11.3%)[d]	0	0	0
ALT, IU/L	2126 ± 938[e,*]	2394 ± 820	2857 ± 1668[e]	4180	1175	1533
Bilirubin, mg/dL	7.1 ± 6.4[f*]	4.8 ± 3.3[f,g]	9.0 ± 7.5[g]	6.8	3.9	3.5
HBV DNA, log copies/mL	6.3 ± 1.7[h,*]	5.5 ± 2.3	4.9 ± 1.5[h]	5.2	7.4	4.8
HBeAg	95/121 (77.3%)[i,*]	24/28 (88.5%)	37/58 (65.5%)[i]	1/1 (100%)	1/1 (100%)	1/1 (100%)
Anti-HIV	7/72 (9.7%)	0/7 (0%)	0/23 (0%)	Not tested	0/1 (0%)	Not tested
Duration of HBsAg*						
Group (mo)						
1 (<3)	35 (42.2%)	16 (64.0%)	31 (64.6%)	0	1	1
2 (3–6)	34 (41.0%)	8 (32.0%)	11 (22.9%)	1	0	0
3 (>6 –12)	9 (10.8%)	0	6 (12.5%)	0	0	0
4 (>12)	5 (6.0%)	1 (4.0%)	0	0	0	0

Abbreviations: ALT, alanine aminotransferase; anti-HIV, antibody to human immunodeficiency virus; HBeAg, hepatitis B e antigen; HBsAg, hepatitis B surface antigen; HBV, hepatitis B virus; MSM, men who have sex with men.

[a] $P < .001$.

[b] $P < .001$.

[c] $P = .017$.

[d] $P = .002$.

[e] $P = .002$.

[f] $P = .003$.

[g] $P < .001$.

[h] $P < .001$.

[i] $P = .036$.

* Data from anti-HIV-positive patients are excluded.

with acute hepatitis B in this study were very close to one another suggests that most HBV/A strains were imported recently and have spread rapidly, which may be attributed to the features of HBV/A in transmission routes and viral kinetics. We have reported that patients with genotype A tend to have multiple sexual partners [5]. Consequently, chances of secondary transmission of HBV/A would be higher than those of other genotypes, which may increase the number of patients who contract HBV/A infections. On the other hand, HBsAg persisted longer in patients with genotype A than B or C, which is consistent with the in vivo experiment using chimera mice carrying human hepatocytes showing that proliferation of HBV starts later and lasts longer in genotype A than in B or C infection [19].

Our results have shown that 6% of the patients with genotype A develop persistent infection. Because liver cirrhosis or hepatocellular carcinoma can develop in a substantial population of HBV carriers [20, 21], it is important to distinguish the patients in whom HBV infection becomes chronic, and follow them carefully. Although polymorphisms in host genes may be useful for identifying patients who are prone to develop chronic HBV infection [22], simple surrogate markers for the outcome have not been reported. Our data indicate that it would be difficult to predict the clinical outcome based on serum levels of viral markers at the first visit alone. This is understandable, because the dose of infecting virus, as well as the interval between infection and the first visit, can vary widely. Hence, we set out to analyze changes in serum levels of viral markers.

As seen in Figure 2, HBsAg levels at 12 weeks from the onset were most useful for discriminating among groups 2, 3, and 4 in the genotype A infection. Therefore, the outcome of acute hepatitis B may be predictable at this time point. Of note is the reelevation of HBsAg observed in group IV (Supplementary Figure 1*A*). Reelevation of viral markers suggests prolonged viral proliferation in the liver, and may be useful to identify the patients who may develop chronic infection.

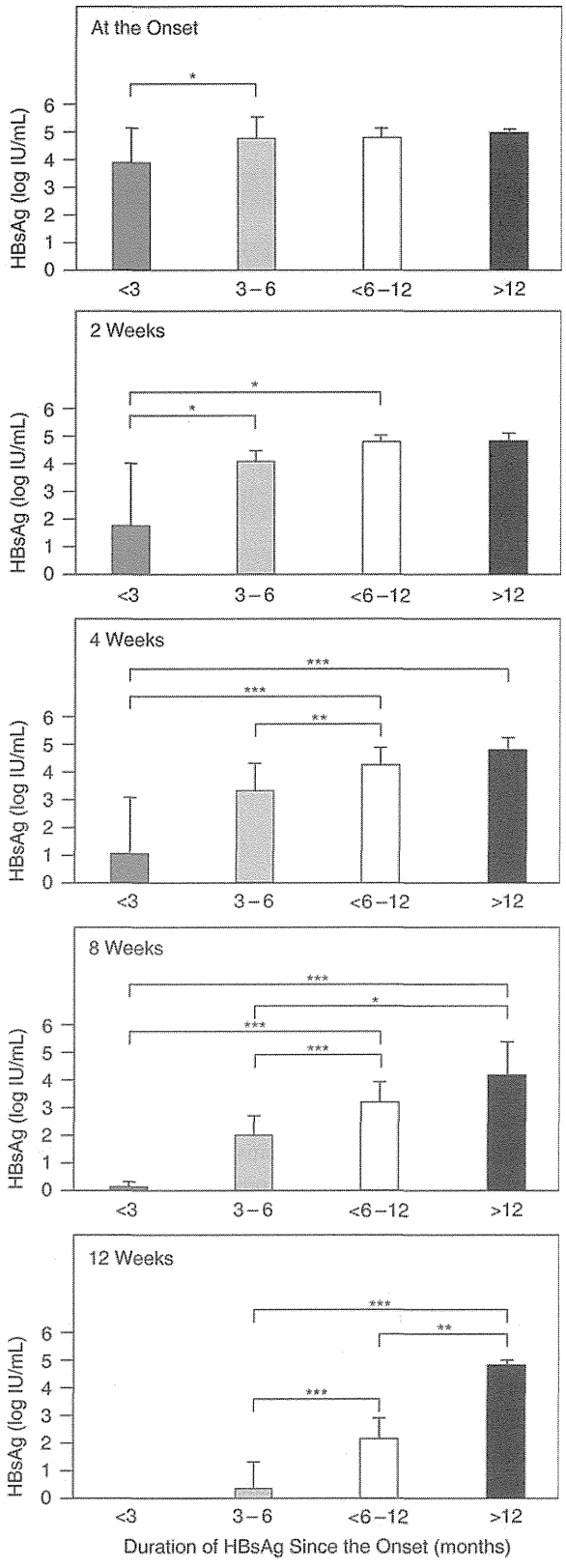

Figure 2. Levels of hepatitis B surface antigen in patients with different durations of infection compared at various weeks after the onset of acute hepatitis B genotype A *$P < .05$; **$P < .01$; ***$P < .001$. Abbreviation: HBsAg, hepatitis B surface antigen.

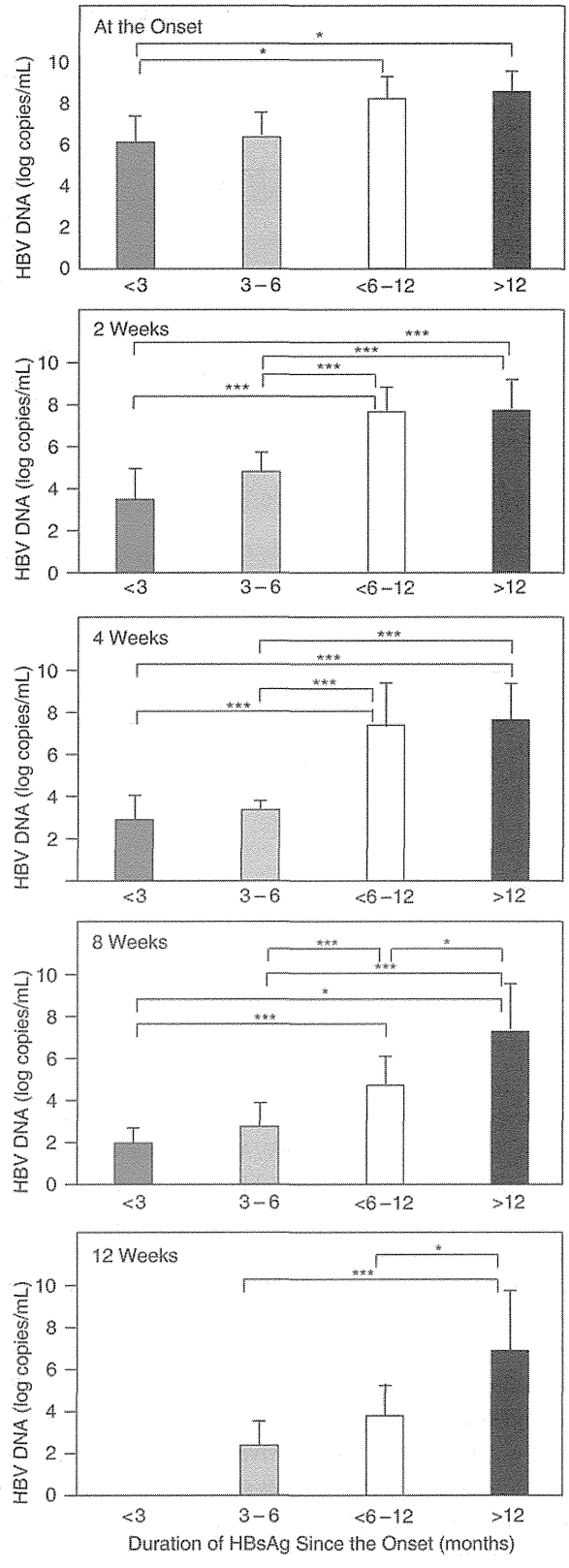

Figure 3. Levels of hepatitis B virus DNA in patients with different durations of infection compared at various weeks after the onset of acute hepatitis B genotype A. *$P < .05$; **$P < .01$; ***$P < .001$. Abbreviations: HBsAg, hepatitis B surface antigen; HBV, hepatitis B virus.

As shown in Figure 3, HBV DNA levels at 4 weeks from the onset can discriminate groups 1/2 from groups 3/4. Furthermore, HBV DNA levels at 8 weeks from the onset can distinguish group 4 from group 1, 2, or 3. Therefore, the combination of HBV DNA levels at weeks 4 and 8 would be useful for predicting the outcome. For the prediction of a chronic outcome, HBV DNA level at 8 weeks from the onset is a useful surrogate marker of the outcome as well as HBsAg level at 12 weeks. There were differences in viral kinetics among groups 1, 2, 3, and 4.

Our present study showed that 15 of the 215 patients (7.0%) cleared HBsAg from >6 to 12 months after the onset. Sixty percent of the 15 patients had HBV/A. Although these patients met the criteria of chronic infection, they finally cleared HBsAg from the sera. Therefore, we would like to propose that transition to chronic infection in acute hepatitis B be judged at 12 months from onset in patients with genotype A; further studies in larger cohorts are necessary. One reason for our proposal is the indication of antiviral treatment. Antiviral treatment in patients with acute hepatitis B is not indicated because previous studies failed to show the efficacy of antiviral treatments in the patients with acute hepatitis B [23, 24]. However, if patients who actually develop chronic infection can be identified and treated by antiviral treatment, the number of those who develop secondary infection may be markedly reduced. Evaluation of the efficacy of antiviral treatments by prospective studies, based on surrogate markers for the outcome, should be conducted as the next step. HBeAg, which was reported to be useful as a surrogate marker for chronicity, should also be assessed as a surrogate marker [25, 26].

Our study has some limitations. First, the lack of data in early stages made it difficult to study viral kinetics precisely. Second, viral kinetics in the infection with each HBV genotype were obtained from a restricted number of patients, not large enough to establish the usefulness of changes in viral markers in earlier stages of HBV infection. Third, anti-HIV was not checked in all patients due to the lack of informed consent. Fourth, HBsAg and HBV DNA were not determined 24 weeks after onset when discrimination between groups 3 and 4 may be possible more easily. Fifth, the maximum levels of ALT and bilirubin may be affected by the time of blood test. Validation studies in larger cohorts are necessary to evaluate the feasibility of our hypotheses.

In conclusion, we have shown that viral kinetics and the clinical outcome are different among patients with acute hepatitis B who are infected with HBV of distinct genotypes. HBsAg levels at 12 weeks and HBV DNA at 8 weeks after the onset would be useful to predict the clinical outcome of patients with acute hepatitis B.

Supplementary Data

Supplementary materials are available at *Clinical Infectious Diseases* online (http://cid.oxfordjournals.org/). Supplementary materials consist of data provided by the author that are published to benefit the reader. The posted materials are not copyedited. The contents of all supplementary data are the sole responsibility of the authors. Questions or messages regarding errors should be addressed to the author.

Notes

Financial support. This work was supported by grants from the Ministry of Health, Labor and Welfare of Japan.

Potential conflicts of interest. All authors: No reported conflicts.

All authors have submitted the ICMJE Form for Disclosure of Potential Conflicts of Interest. Conflicts that the editors consider relevant to the content of the manuscript have been disclosed.

References

1. Kusakabe A, Tanaka Y, Mochida S, et al. Case-control study for the identification of virological factors associated with fulminant hepatitis B. Hepatol Res **2009**; 39:648–56.
2. Mayerat C, Mantegani A, Frei PC. Does hepatitis B virus (HBV) genotype influence the clinical outcome of HBV infection? J Viral Hepat **1999**; 6:299–304.
3. Tamada Y, Yatsuhashi H, Masaki N, et al. Hepatitis B virus strains of subgenotype A2 with an identical sequence spreading rapidly from the capital region to all over Japan in patients with acute hepatitis B. Gut **2012**; 61:765–73.
4. Kobayashi M, Arase Y, Ikeda K, et al. Clinical features of hepatitis B virus genotype A in Japanese patients. J Gastroenterol **2003**; 38:656–62.
5. Yotsuyanagi H, Okuse C, Yasuda K, et al. Distinct geographic distributions of hepatitis B virus genotypes in patients with acute infection in Japan. J Med Virol **2005**; 77:39–46.
6. Zhang HW, Yin JH, Li YT, et al. Risk factors for acute hepatitis B and its progression to chronic hepatitis in Shanghai, China. Gut **2008**; 57: 1713–20.
7. Reijnders JG, Rijckborst V, Sonneveld MJ, et al. Kinetics of hepatitis B surface antigen differ between treatment with peginterferon and entecavir. J Hepatol **2011**; 54:449–54.
8. Sonneveld MJ, Rijckborst V, Boucher CA, Hansen BE, Janssen HL. Prediction of sustained response to peginterferon alfa-2b for hepatitis B e antigen-positive chronic hepatitis B using on-treatment hepatitis B surface antigen decline. Hepatology **2010**; 52:1251–7.
9. Wursthorn K, Jung M, Riva A, et al. Kinetics of hepatitis B surface antigen decline during 3 years of telbivudine treatment in hepatitis B e antigen-positive patients. Hepatology **2010**; 52:1611–20.
10. Brunetto MR, Oliveri F, Colombatto P, et al. Hepatitis B surface antigen serum levels help to distinguish active from inactive hepatitis B virus genotype D carriers. Gastroenterology **2010**; 139:483–90.
11. Jaroszewicz J, Calle Serrano B, Wursthorn K, et al. Hepatitis B surface antigen (HBsAg) levels in the natural history of hepatitis B virus (HBV) infection: a European perspective. J Hepatol **2010**; 52:514–22.
12. Kato H, Orito E, Sugauchi F, et al. Frequent coinfection with hepatitis B virus strains of distinct genotypes detected by hybridization with type-specific probes immobilized on a solid-phase support. J Virol Methods **2003**; 110:29–35.
13. Yano K, Tamada Y, Yatsuhashi H, et al. Dynamic epidemiology of acute viral hepatitis in Japan. Intervirology **2010**; 53:70–5.
14. Matsuura K, Tanaka Y, Hige S, et al. Distribution of hepatitis B virus genotypes among patients with chronic infection in Japan shifting toward an increase of genotype A. J Clin Microbiol **2009**; 47:1476–83.
15. Gojobori T, Ishii K, Nei M. Estimation of average number of nucleotide substitutions when the rate of substitution varies with nucleotide. J Mol Evol **1982**; 18:414–23.
16. Saitou N, Nei M. The neighbor-joining method: a new method for reconstructing phylogenetic trees. Mol Biol Evol **1987**; 4:406–25.
17. Felsenstein J. Confidence limits on phylogenesis, an approach using the bootstrap. Evolution **1985**; 39:783–91.

18. Ogawa M, Hasegawa K, Naritomi T, Torii N, Hayashi N. Clinical features and viral sequences of various genotypes of hepatitis B virus compared among patients with acute hepatitis B. Hepatol Res **2002**; 23: 167–77.
19. Sugiyama M, Tanaka Y, Kurbanov F, et al. Direct cytopathic effects of particular hepatitis B virus genotypes in severe combined immunodeficiency transgenic with urokinase-type plasminogen activator mouse with human hepatocytes. Gastroenterology **2009**; 136:652–62. e3.
20. McMahon BJ, Holck P, Bulkow L, Snowball M. Serologic and clinical outcomes of 1536 Alaska Natives chronically infected with hepatitis B virus. Ann Intern Med **2001**; 135:759–68.
21. Chu CM. Natural history of chronic hepatitis B virus infection in adults with emphasis on the occurrence of cirrhosis and hepatocellular carcinoma. J Gastroenterol Hepatol **2000**; 15(suppl):E25–30.
22. Kamatani Y, Wattanapokayakit S, Ochi H, et al. A genome-wide association study identifies variants in the *HLA-DP* locus associated with chronic hepatitis B in Asians. Nat Genet **2009**; 41:591–5.
23. Kumar M, Satapathy S, Monga R, et al. A randomized controlled trial of lamivudine to treat acute hepatitis B. Hepatology **2007**; 45:97–101.
24. Tassopoulos NC, Koutelou MG, Polychronaki H, Paraloglou-Ioannides MHadziyannis SJ. Recombinant interferon-alpha therapy for acute hepatitis B: a randomized, double-blind, placebo-controlled trial. J Viral Hepat **1997**; 4:387–94.
25. Aldershvile J, Frösner GG, Nielsen JO, et al. Hepatitis B e antigen and antibody measured by radioimmunoassay in acute hepatitis B surface antigen-positive hepatitis. J Infect Dis **1980**; 141:293–8.
26. Aldershvile J, Nielsen JO. HBeAg, anti-HBe and anti-HBc IgM in patients with hepatitis B. J Virol Methods **1980**; 2:97–105.

Cell

Identification of Liver Cancer Progenitors Whose Malignant Progression Depends on Autocrine IL-6 Signaling

Guobin He,[1,13] Debanjan Dhar,[1,13] Hayato Nakagawa,[1,11,13] Joan Font-Burgada,[1,13] Hisanobu Ogata,[1,12,13] Yuhong Jiang,[1] Shabnam Shalapour,[1] Ekihiro Seki,[2] Shawn E. Yost,[4,5] Kristen Jepsen,[5] Kelly A. Frazer,[5,6,7,8] Olivier Harismendy,[5,6,7] Maria Hatziapostolou,[9] Dimitrios Iliopoulos,[9] Atsushi Suetsugu,[3,10] Robert M. Hoffman,[3,10] Ryosuke Tateishi,[11] Kazuhiko Koike,[11] and Michael Karin[1,6,*]

[1]Laboratory of Gene Regulation and Signal Transduction, Departments of Pharmacology and Pathology
[2]Department of Medicine
[3]Department of Surgery
[4]Bioinformatics Graduate Program
[5]Rady's Children's Hospital and Department of Pediatrics
[6]Moores UCSD Cancer Center
[7]Clinical and Translational Research Institute
[8]Institute for Genomic Medicine
University of California San Diego, School of Medicine, 9500 Gilman Drive, San Diego, CA 92093, USA
[9]Center for Systems Biomedicine, Division of Digestive Diseases and Institute for Molecular Medicine, David Geffen School of Medicine, University of California Los Angeles, Los Angeles, CA 90095, USA
[10]AntiCancer, Inc., San Diego, CA 92111, USA
[11]Department of Gastroenterology, University of Tokyo, Tokyo 113-8655, Japan
[12]Department of Medicine and Clinical Science, Graduate School of Medical Sciences, Kyushu University, Fukuoka 812-8582, Japan
[13]These authors contributed equally to this work
*Correspondence: karinoffice@ucsd.edu
http://dx.doi.org/10.1016/j.cell.2013.09.031

SUMMARY

Hepatocellular carcinoma (HCC) is a slowly developing malignancy postulated to evolve from premalignant lesions in chronically damaged livers. However, it was never established that premalignant lesions actually contain tumor progenitors that give rise to cancer. Here, we describe isolation and characterization of HCC progenitor cells (HcPCs) from different mouse HCC models. Unlike fully malignant HCC, HcPCs give rise to cancer only when introduced into a liver undergoing chronic damage and compensatory proliferation. Although HcPCs exhibit a similar transcriptomic profile to bipotential hepatobiliary progenitors, the latter do not give rise to tumors. Cells resembling HcPCs reside within dysplastic lesions that appear several months before HCC nodules. Unlike early hepatocarcinogenesis, which depends on paracrine IL-6 production by inflammatory cells, due to upregulation of LIN28 expression, HcPCs had acquired autocrine IL-6 signaling that stimulates their in vivo growth and malignant progression. This may be a general mechanism that drives other IL-6-producing malignancies.

INTRODUCTION

Every malignant tumor is probably derived from a single progenitor that had acquired growth and survival advantages through genetic and epigenetic changes, allowing clonal expansion (Nowell, 1976). Tumor progenitors are not necessarily identical to cancer stem cells (CSCs), which maintain and renew fully established malignancies (Nguyen et al., 2012). However, clonal evolution and selective pressure may cause some descendants of the initial progenitor to cross the bridge of no return and form a premalignant lesion. Cancer genome sequencing indicates that most cancers require at least five genetic changes to evolve (Wood et al., 2007). How these changes affect the properties of tumor progenitors and control their evolution into a CSC is not entirely clear, as it has been difficult to isolate and propagate cancer progenitors prior to detection of tumor masses. Given these difficulties, it is also not clear whether cancer progenitors are the precursors for the more malignant CSC isolated from fully established cancers. An answer to these critical questions depends on identification and isolation of cancer progenitors, which may also enable definition of molecular markers and signaling pathways suitable for early detection and treatment. This is especially important in cancers of the liver and pancreas, which evolve over the course of many years but, once detected, are extremely difficult to treat (El-Serag, 2011; Hruban et al., 2007).

Hepatocellular carcinoma (HCC), the most common liver cancer, is the end product of chronic liver diseases, requiring

several decades to evolve (El-Serag, 2011). Currently, HCC is the third most deadly and fifth most common cancer worldwide, and in the United States its incidence has doubled in the past two decades. Furthermore, 8% of the world's population are chronically infected with hepatitis B or C viruses (HBV and HCV) and are at a high risk of new HCC development (El-Serag, 2011). Up to 5% of HCV patients will develop HCC in their lifetime, and the yearly HCC incidence in patients with cirrhosis is 3%–5%. These tumors may arise from premalignant lesions, ranging from dysplastic foci to dysplastic hepatocyte nodules that are often seen in damaged and cirrhotic livers and are more proliferative than the surrounding parenchyma (Hytiroglou et al., 2007). However, the tumorigenic potential of these lesions was never examined, and it is unknown whether they contain any genetic alterations. Given that there is no effective treatment for HCC and, upon diagnosis, most patients with advanced disease have a remaining lifespan of 4–6 months, it is important to detect HCC early, while it is still amenable to surgical resection or chemotherapy. Premalignant lesions, called foci of altered hepatocytes (FAH), were also described in chemically induced HCC models (Pitot, 1990), but it was questioned whether these lesions harbor tumor progenitors or result from compensatory proliferation (Sell and Leffert, 2008). The aim of this study was to determine whether HCC progenitor cells (HcPCs) exist and if so, to isolate these cells and identify some of the signaling networks that are involved in their maintenance and progression.

We now describe HcPC isolation from mice treated with the procarcinogen diethyl nitrosamine (DEN), which induces poorly differentiated HCC nodules within 8 to 9 months (Verna et al., 1996). Although these tumors do not evolve in the context of cirrhosis, the use of a chemical carcinogen is justified because the finding of up to 121 mutations per HCC genome suggests that carcinogens may be responsible for human HCC induction (Guichard et al., 2012). Furthermore, 20%–30% of HCC, especially in HBV-infected individuals, evolve in noncirrhotic livers (El-Serag, 2011). Nonetheless, we also isolated HcPCs from *Tak1*$^{\Delta hep}$ mice, which develop spontaneous HCC as a result of progressive liver damage, inflammation, and fibrosis caused by ablation of TAK1 (Inokuchi et al., 2010). Although the etiology of each model is distinct, both contain HcPCs that express marker genes and signaling pathways previously identified in human HCC stem cells (Marquardt and Thorgeirsson, 2010) long before visible tumors are detected. Furthermore, DEN-induced premalignant lesions and HcPCs exhibit autocrine IL-6 production that is critical for tumorigenic progression. Circulating IL-6 is a risk indicator in several human pathologies and is strongly correlated with adverse prognosis in HCC and cholangiocarcinoma (Porta et al., 2008; Soresi et al., 2006). IL-6 produced by in-vitro-induced CSCs was suggested to be important for their maintenance (Iliopoulos et al., 2009). Furthermore, autocrine IL-6 was detected in several cancers, but its origin is poorly understood (Grivennikov and Karin, 2008). In particular, little is known about the source of IL-6 in HCC. In early stages of hepatocarcinogenesis, IL-6 is produced by Kupffer cells or macrophages (Maeda et al., 2005; Naugler et al., 2007). However, paracrine IL-6 production is transient and does not explain its expression by HCC cells.

RESULTS

DEN-Induced Collagenase-Resistant Aggregates of HCC Progenitors

A single intraperitoneal (i.p.) injection of DEN into 15-day-old BL/6 mice induces HCC nodules first detected 8 to 9 months later. However, hepatocytes prepared from macroscopically normal livers 3 months after DEN administration already contain cells that progress to HCC when transplanted into the permissive liver environment of MUP-uPA mice (He et al., 2010), which express urokinase plasminogen activator (uPA) from a mouse liver-specific major urinary protein (MUP) promoter and undergo chronic liver damage and compensatory proliferation (Rhim et al., 1994). Collagenase digestion of DEN-treated livers generated a mixture of monodisperse hepatocytes and aggregates of tightly packed small hepatocytic cells (Figure 1A). Aggregated cells were also present—but in lower abundance—in digests of control livers (Figure S1A available online). HCC markers such as α fetoprotein (AFP), glypican 3 (Gpc3), and Ly6D, whose expression in mouse liver cancer was reported (Meyer et al., 2003), were upregulated in aggregates from DEN-treated livers, but not in nonaggregated hepatocytes or aggregates from control livers (Figure S1A). Thus, control liver aggregates may result from incomplete collagenase digestion, whereas aggregates from DEN-treated livers may contain HcPC. DEN-induced aggregates became larger and more abundant 5 months after carcinogen exposure, when they consisted of 10–50 cells that were smaller than nonaggregated hepatocytes. Using 70 μm and 40 μm sieves, we separated aggregated from nonaggregated hepatocytes (Figure 1A) and tested their tumorigenic potential by transplantation into MUP-uPA mice (Figure 1B). To facilitate transplantation, the aggregates were mechanically dispersed and suspended in Dulbecco's modified Eagle's medium (DMEM). Five months after intrasplenic (i.s.) injection of 10^4 viable cells, mice receiving cells from aggregates developed about 18 liver tumors per mouse, whereas mice receiving nonaggregated hepatocytes developed less than 1 tumor each (Figure 1B). The tumors exhibited typical trabecular HCC morphology and contained cells that abundantly express AFP (Figure S1B). To confirm that the HCCs were derived from transplanted cells, we measured their relative MUP-uPA DNA copy number and found that they contained much less MUP-uPA transgene DNA than the surrounding parenchyma (Figure S1C). Transplantation of aggregated cells from livers of DEN-treated actin-GFP transgenic mice resulted in GFP-positive HCCs (Figure S1D). Both experiments strongly suggest that the HCCs were derived from the transplanted cells. No tumors were ever observed after transplantation of control hepatocytes (nonaggregated or aggregated).

Only liver tumors were formed by the transplanted cells. Other organs, including the spleen into which the cells were injected, remained tumor free (Figure 1B), suggesting that HcPCs progress to cancer only in the proper microenvironment. Indeed, no tumors appeared after HcPC transplantation into normal BL/6 mice. But, if BL/6 mice were first treated with retrorsine (a chemical that permanently inhibits hepatocyte proliferation [Laconi et al., 1998]), intrasplenically transplanted with HcPC-containing aggregates, and challenged with CCl_4 to induce liver injury and compensatory proliferation (Guo et al., 2002), HCCs readily

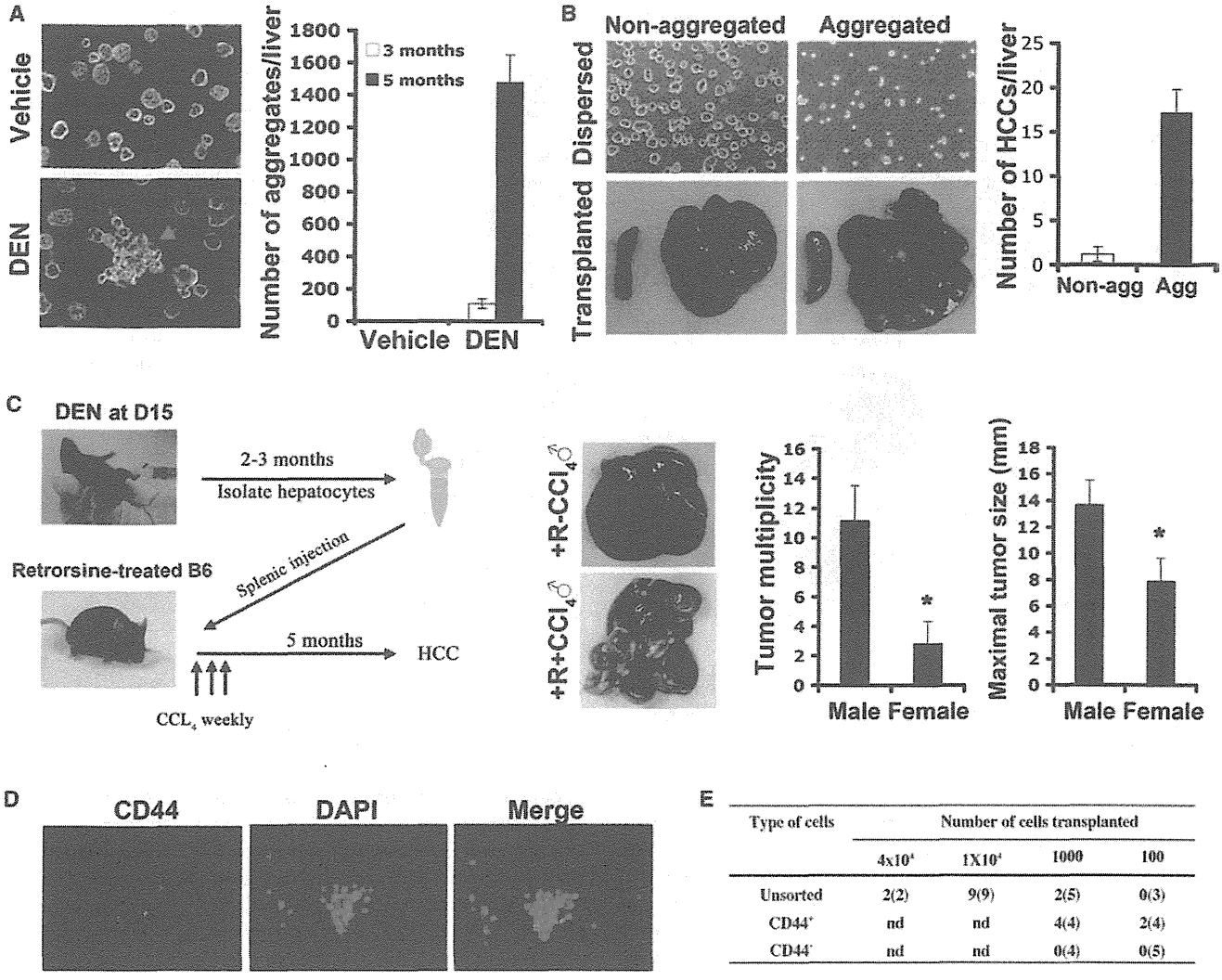

E

Type of cells	Number of cells transplanted			
	$4x10^4$	$1X10^4$	1000	100
Unsorted	2(2)	9(9)	2(5)	0(3)
$CD44^+$	nd	nd	4(4)	2(4)
$CD44^-$	nd	nd	0(4)	0(5)

Figure 1. DEN-Induced Hepatocytic Aggregates Contain $CD44^+$ HCC Progenitors

(A) Fifteen-day-old BL/6 males were given DEN or vehicle. After 3 or 5 months, their livers were removed and collagenase digested. Left: typical digest appearance (magnification: 400×; 3 months after DEN). Red arrow indicates a collagenase-resistant aggregate. Right: aggregates per liver (n = 5; ± SD for each point).

(B) Livers were collagenase digested 5 months after DEN administration. Aggregates were separated from nonaggregated cells and mechanically dispersed into a single-cell suspension (left upper panels; 200×). 10^4 viable aggregated or nonaggregated cells were i.s. injected into MUP-uPA mice whose livers and spleens were analyzed for tumors 5 months later (left lower panels). The number of HCC nodules per liver was determined (n = 5; ± SD).

(C) Adult BL/6 mice were given retrorsine twice with a 2 week interval to inhibit hepatocyte proliferation. After 1 month, mice were i.s. transplanted with dispersed hepatocyte aggregates (10^4 cells) from DEN-treated mice and, 2 weeks later, were given three weekly i.p. injections of CCl_4 or vehicle. Tumor multiplicity and size were evaluated 5 months later (n = 5; ± SD).

(D) Hepatocyte aggregates were prepared as in (A), stained with CD44 antibody and DAPI, and examined by fluorescent microscopy (400×).

(E) Hepatocyte aggregates were dispersed as above, and $CD44^+$ cells were separated from $CD44^-$ cells. The indicated cell numbers were injected into MUP-uPA mice, and HCC development was evaluated 5 months later. n values are in parentheses (n.d., not done).

See also Figure S1.

appeared (Figure 1C). CCl_4 omission prevented tumor development. Notably, MUP-uPA or CCl_4-treated livers are fragile, rendering direct intrahepatic transplantation difficult. The transplanted HcPC-containing aggregates formed more numerous and larger HCC nodules in male recipients than in females (Figure 1C), as observed in MUP-uPA mice transplanted with unfractionated DEN-exposed hepatocytes (He et al., 2010). Thus, CCl_4-induced liver damage, especially within a male liver, generates a microenvironment that drives HcPC proliferation and malignant progression. To examine this point, we transplanted GFP-labeled HcPC-containing aggregates into retrorsine-treated BL/6 mice and examined their ability to proliferate with or without subsequent CCl_4 treatment. Indeed, the GFP^+ cells formed clusters that grew in size only in CCl_4-treated host livers

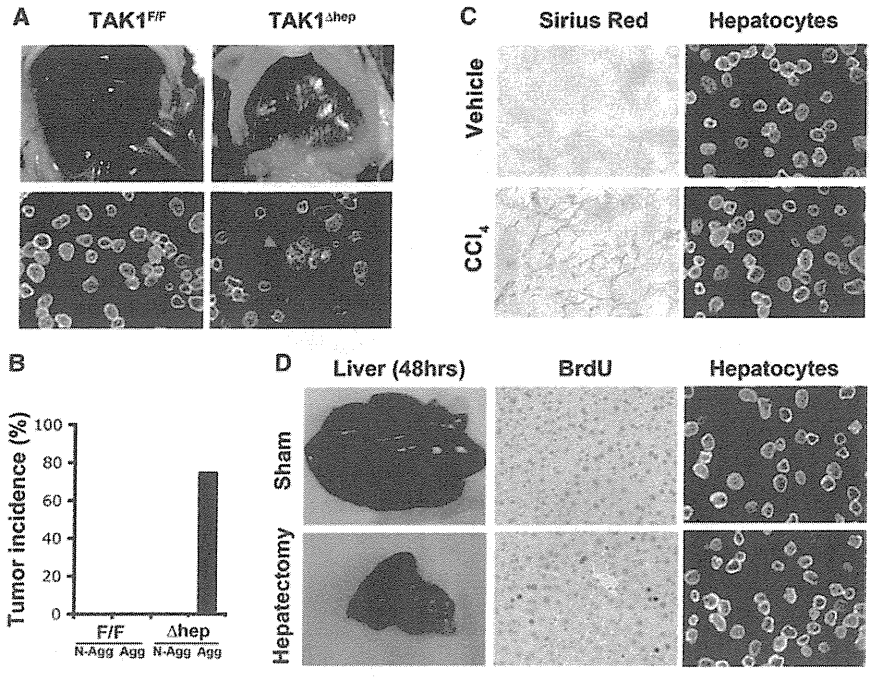

Figure 2. *Tak1*$^{\Delta hep}$ Livers Contain Collagenase-Resistant HcPC Aggregates

(A) Livers, free of tumors (upper panels), were removed from 1-month-old *Tak1*$^{F/F}$ and *Tak1*$^{\Delta hep}$ males and collagenase digested (lower panels; red arrow indicates collagenase-resistant aggregate).

(B) 10^4 nonaggregated or dispersed aggregated hepatocytes from (A) were i.s. injected into MUP-uPA mice that were analyzed 6 months later to identify mice with at least one liver tumor (n = 5–8 mice per genotype).

(C) BL/6 males were injected with vehicle or CCl_4 twice weekly for 2 weeks. Hepatocytes were isolated by collagenase digestion and photographed (right panels; 400×). Liver sections were stained with Sirius red to reveal collagen deposits (left panels).

(D) 8-week-old BL/6 males were subjected to 70% partial hepatectomy, pulsed with BrdU at 46 and 70 hr, and sacrificed 2 hr later. Isolated hepatocytes were photographed. Liver sections were analyzed for BrdU incorporation (400×). See also Figure S2 and Table S1.

(Figure S1E). Omission of $CC1_4$ prevented their expansion. Unlike HCC-derived cancer cells (dih10 cells), which form subcutaneous (s.c.) tumors with HCC morphology (He et al., 2010; Park et al., 2010), the HcPC-containing aggregates did not generate s.c. tumors in BL/6 mice (Figure S1F).

Despite their homogeneous appearance, the HcPC-containing aggregates contained both $CD44^+$ and $CD44^-$ cells (Figure 1D). Because CD44 is expressed by HCC stem cells (Yang et al., 2008; Zhu et al., 2010), we dispersed the aggregates and separated $CD44^+$ from $CD44^-$ cells and transplanted both into MUP-uPA mice. Whereas as few as 10^3 $CD44^+$ cells gave rise to HCCs in 100% of recipients, no tumors were detected after transplantation of $CD44^-$ cells (Figure 1E). Remarkably, 50% of recipients developed at least one HCC after receiving as few as 10^2 $CD44^+$ cells. Mature $CD44^-$ hepatocytes were found to engraft as well as or better than $CD44^+$ small hepatocytic cells (Haridass et al., 2009; Ichinohe et al., 2012). Hence, livers of DEN-treated mice contain $CD44^+$ HcPC that can be successfully isolated and purified and give rise to HCCs after transplantation into appropriate hosts. Unlike fully transformed HCC cells, HcPCs only give rise to tumors within the liver.

HcPC-Containing Aggregates in *Tak1*$^{\Delta hep}$ Mice

We applied the same HcPC isolation protocol to *Tak1*$^{\Delta hep}$ mice, which develop HCC of different etiology from DEN-induced HCC. Importantly, *Tak1*$^{\Delta hep}$ mice develop HCC as a consequence of chronic liver injury and fibrosis without carcinogen or toxicant exposure (Inokuchi et al., 2010). Indeed, whole-tumor exome sequencing revealed that DEN-induced HCC contained about 24 mutations per 10^6 bases (Mb) sequenced, with *B-Raf*^{V637E} being the most recurrent, whereas 1.4 mutations per Mb were detected in *Tak1*$^{\Delta hep}$ HCC's exome (Table S1). By contrast, *Tak1*$^{\Delta hep}$ HCC exhibited gene copy number changes.

Collagenase digests of 1-month-old *Tak1*$^{\Delta hep}$ livers contained much more hepatocytic aggregates than *Tak1*$^{f/f}$ liver digests (Figure 2A). Notably, HCC developed in 75% of MUP-uPA mice that received dispersed *Tak1*$^{\Delta hep}$ aggregates, but no tumors appeared in mice receiving nonaggregated *Tak1*$^{\Delta hep}$ or total *Tak1*$^{f/f}$ hepatocytes (Figure 2B). Because *Tak1*$^{\Delta hep}$ mice are subject to chronic liver damage and consequent compensatory proliferation, we wanted to ascertain that the HcPCs are not simply proliferating hepatocytes or expanding bipotential hepatobiliary progenitors using CCl_4 to induce liver injury and compensatory proliferation in WT mice. Although this treatment caused acute liver fibrosis, it did not augment formation of collagenase-resistant aggregates (Figure 2C). Similarly, few aggregates were detected in collagenase digests of livers after partial hepatectomy (Figure 2D). However, bile duct ligation (BDL) or feeding with 3,5-dicarbethoxy-1,4-dihydrocollidine (DDC), treatments that cause cholestatic liver injuries and oval cell expansion (Dorrell et al., 2011), did increase the number of small hepatocytic cell aggregates (Figure S2A). Nonetheless, no tumors were observed 5 months after injection of such aggregates into MUP-uPA mice (Figure S2B). Thus, not all hepatocytic aggregates contain HcPCs, and HcPCs only appear under tumorigenic conditions.

The HcPC Transcriptome Is Similar to that of HCC and Oval Cells

To determine the relationship between DEN-induced HcPCs, normal hepatocytes, and fully transformed HCC cells, we analyzed the transcriptomes of aggregated and nonaggregated hepatocytes from male littermates 5 months after DEN administration, HCC epithelial cells from DEN-induced tumors, and normal hepatocytes from age- and gender-matched littermate controls. Clustering analysis distinguished the HCC samples from other samples and revealed that the aggregated

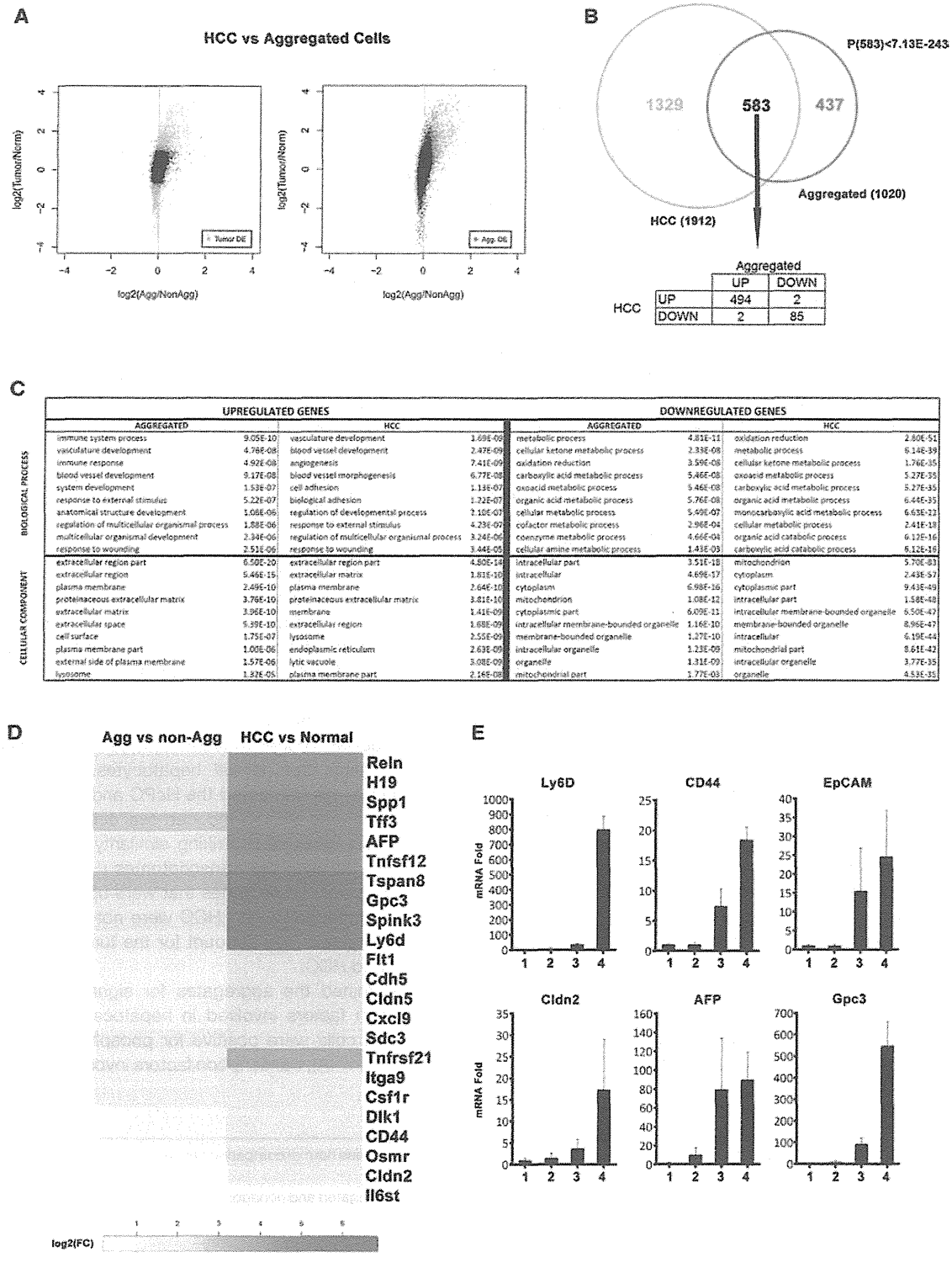

Figure 3. Aggregated Hepatocytes Exhibit an Altered Transcriptome Similar to that of HCC Cells

Aggregated and matched nonaggregated hepatocytes were isolated 5 months after DEN treatment. HCC cells were isolated from DEN-induced tumors, and normal hepatocytes were from age- and gender-matched control mice. RNA was extracted and subjected to microarray analysis (n = 3 for each sample).

(A) Scatterplot representing fold changes (log 2 of expression ratio) in gene expression for HCC versus normal (y axis) and aggregated versus nonaggregated (x axis) pairwise transcriptome comparisons. The plot is displayed twice: in the left panel, genes with an FDR < 0.01 in the aggregated versus nonaggregated

(legend continued on next page)

hepatocyte samples did not cluster with each other but rather with nonaggregated hepatocytes derived from the same mouse (Figure S3A). Interestingly, the aggregated cell transcriptome appeared closer to that of normal hepatocytes than to the HCC profile. This similarity may be due to the presence of ~70% nontumorigenic (or $CD44^-$) hepatocytes within the purified aggregates (Figure 1D). Comparison of the HCC and normal hepatocyte transcriptomes revealed 1,912 differentially expressed genes (false discovery rate [FDR] < 0.01; Figure 3A, left, cyan dots). A similar comparison revealed 1,020 genes that are differentially expressed between aggregated and nonaggregated hepatocytes (FDR < 0.01; Figure 3A, right, red dots). The range of differential expression is wider for the HCC and normal hepatocyte pair than the aggregate versus nonaggregate pair, reflecting presence of normal, nontransformed hepatocytes within the aggregates, resulting in signal dilution. Interestingly, 57% (583/1,020) of genes differentially expressed in aggregated relative to nonaggregated hepatocytes are also differentially expressed in HCC relative to normal hepatocytes (Figure 3B, top), a value that is highly significant ($p < 7.13 \times 10^{-243}$). More specifically, 85% (494/583) of these genes are overexpressed in both HCC and HcPC-containing aggregates (Figure 3B, bottom table). Thus, hepatocyte aggregates isolated 5 months after DEN injection contain cells that are related in their gene expression profile to HCC cells isolated from fully developed tumor nodules.

To gain insight into the functional differences between the transcriptomes of the four populations, we examined which biological processes or cellular compartments were significantly overrepresented in the induced or repressed genes in both pairwise comparisons (Gene Ontology Analysis). As expected, processes and compartments that were enriched in aggregated hepatocytes relative to nonaggregated hepatocytes were almost identical to those that were enriched in HCC relative to normal hepatocytes (Figure 3C). Upregulated genes were related to immune response, angiogenesis, development, and wound healing, and many encoded plasma membrane or secreted proteins. By contrast, downregulated genes were highly enriched for metabolic processes, and many of them encoded mitochondrial proteins or had functions associated with differentiated hepatocytes (Figure 3C). Several human HCC markers, including AFP, Gpc3 and H19, were upregulated in aggregated hepatocytes (Figures 3D and 3E). Aggregated hepatocytes also expressed more Tetraspanin 8 (Tspan8), a cell-surface glycoprotein that complexes with integrins and is overexpressed in human carcinomas (Zöller, 2009). Another cell-surface molecule highly expressed in aggregated cells is Ly6D (Figures 3D and 3E). Immunofluorescence (IF) analysis revealed that Ly6D was undetectable in normal liver but was elevated in FAH and ubiquitously expressed in most HCC cells (Figure S3C). A fluorescent-labeled Ly6D antibody injected into HCC-bearing mice specifically stained tumor nodules (Figure S3D). Other cell-surface molecules that were upregulated in aggregated cells included syndecan 3 (Sdc3), integrin α 9 (Itga9), claudin 5 (Cldn5), and cadherin 5 (Cdh5) (Figure 3D). Aggregated hepatocytes also exhibited elevated expression of extracellular matrix proteins (TIF3 and Reln1) and a serine protease inhibitor (Spink3). Elevated expression of such proteins may explain aggregate formation. Aggregated hepatocytes also expressed progenitor cell markers, including the epithelial cell adhesion molecule (EpCAM) (Figure 3E) and Dlk1 (Figure 3D). Elevated expression of cytokines and cytokine receptors was also detected, including tumor necrosis factor superfamily members 12 and 21, colony-stimulating factor 1 receptor, FMS-like tyrosine kinase 1, chemokine (C-X-C motif) ligand 9, the STAT3-activating cytokine osteopontin, IL-6 receptor (IL-6R) signal transducing subunit (gp130), and oncostatin M (OSM) receptor, which also activates STAT3 (Figure 3D).

Aggregated hepatocytes expressed albumin, albeit less than nonaggregated hepatocytes (Figure 4A). Some aggregated cells were positive for cytokeratin 19 (CK19) and A6, markers for bile duct epithelium and oval cells (Figure 4A). Most cells in the DEN-induced aggregates were AFP positive, and some of them expressed EpCAM (Figure 4A). However, not all markers were expressed by every cell within a given aggregate, suggesting that the aggregates contain liver cells that are related to bipotential hepatobiliary progenitors/oval cells as well as more differentiated progeny and normal hepatocytes. To confirm these observations, we compared the HcPC and HCC (Figure 3A) to the transcriptome of DDC-induced oval cells (Shin et al., 2011). This analysis revealed a striking similarity between the HCC, HcPC, and the oval cell transcriptomes (Figure S3B). Despite these similarities, some genes that were upregulated in HcPC-containing aggregates and HCC were not upregulated in oval cells. Such genes may account for the tumorigenic properties of HcPC and HCC.

We examined the aggregates for signaling pathways and transcription factors involved in hepatocarcinogenesis. Many aggregated cells were positive for phosphorylated c-Jun and STAT3 (Figure 4A), transcription factors involved in DEN-induced

comparison are highlighted in red, and in the right panel, genes with an FDR < 0.01 in the HCC versus normal comparison are highlighted in cyan. DE, differentially expressed.

(B) Venn diagram showing overlap between genes that are differentially expressed between aggregated and nonaggregated hepatocytes and between HCC cells and normal hepatocytes with an FDR < 0.01 (cyan and red dots from A). The probability to find 583 overlapping genes is $<7.13 \times 10^{-243}$. From these 583 common genes, only 4 behaved differently.

(C) The ten most enriched biological processes (upper table) and cellular compartments (lower panel) represented by genes that are significantly upregulated (left panel) or downregulated (right panel) in HCC relative to normal hepatocytes (HCC) or in aggregated relative to nonaggregated hepatocytes (aggregated).

(D) Heatmap displaying positive fold changes (FC) in expression of genes of interest in aggregated versus nonaggregated HcPCs (left) and in HCC versus normal hepatocytes (right).

(E) Expression of selected genes was examined by real-time PCR and is depicted as fold change relative to normal hepatocytes given an arbitrary value of 1.0 (n = 3; ± SD). (1) Normal hepatocytes; (2) nonaggregated hepatocytes from DEN-treated liver; (3) HcPC aggregates from DEN-treated liver; and (4) DEN-induced HCCs.

See also Figure S3.

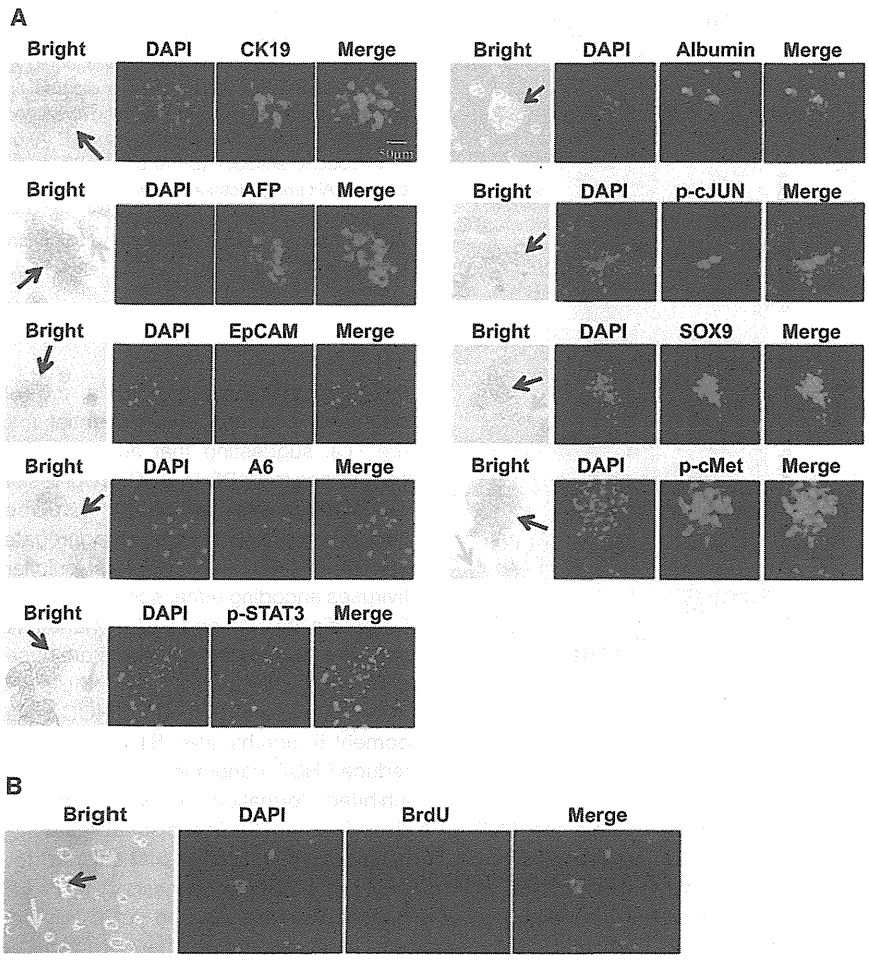

Figure 4. DEN-Induced HcPC Aggregates Express Pathways and Markers Characteristic of HCC and Hepatobiliary Stem Cells

(A) Cytospin preps of collagenase-resistant aggregates from 5-month-old DEN-injected mice were stained with antibodies to CK19, AFP, EpCAM, A6, phospho-Y-STAT3 (Tyr705), albumin, phospho-c-Jun, Sox9, and phospho-c-Met. Black arrows indicate aggregates, and yellow arrows indicate nonaggregated cells (magnification: 400×). (B) 5-month-old DEN-treated mice were injected with BrdU, and 2 hr later, collagenase-resistant aggregates were isolated and analyzed for BrdU incorporation (400×).

See also Figure S4.

hepatocarcinogenesis (Eferl et al., 2003; He et al., 2010). Sox9, a transcription factor that marks hepatobiliary progenitors (Dorrell et al., 2011), was also expressed by many of the aggregated cells, which were also positive for phosphorylated c-Met (Figure 4A), a receptor tyrosine kinase that is activated by hepatocyte growth factor (HGF) and is essential for liver development (Bladt et al., 1995) and hepatocarcinogenesis (Wang et al., 2001). Few of the nonaggregated hepatocytes exhibited activation of these signaling pathways. Aggregates from bromodeoxyuridine (BrdU)-pulsed DEN-treated mice contained BrdU-positive cells (Figure 4B), indicating that they were actively proliferating prior to isolation. Hepatocyte aggregates from 1-month-old *Tak1*$^{\Delta hep}$ mice also contained cells positive for AFP, Sox9, phosphorylated c-Met, and EpCAM, but not A6-positive cells (Figure S4A). Many of the cells also exhibited partially activated β-catenin, phosphorylated STAT3, and phosphorylated c-Jun. Thus, despite different etiology, HcPC-containing aggregates from *Tak1*$^{\Delta hep}$ mice exhibit upregulation of many of the same markers and pathways that are upregulated in DEN-induced HcPC-containing aggregates. Flow cytometry confirmed enrichment of CD44$^+$ cells as well as CD44$^+$/CD90$^+$ and CD44$^+$/EpCAM$^+$ double-positive cells in the HcPC-containing aggregates from either DEN-treated or *Tak1*$^{\Delta hep}$ livers (Figure S4B).

HcPC-Containing Aggregates Originate from Premalignant Dysplastic Lesions

FAH are dysplastic lesions occurring in rodent livers exposed to hepatic carcinogens (Su et al., 1990). Similar lesions are present in premalignant human livers (Su et al., 1997). Yet, it is still debated whether FAH correspond to premalignant lesions or are a reaction to liver injury that does not lead to cancer (Sell and Leffert, 2008). In DEN-treated males, FAH were detected as early as 3 months after DEN administration (Figure 5A), concomitant with the time at which HcPC-containing aggregates were detected. In females, FAH development was delayed. In both genders, FAH were confined to zone 3 and consisted of tightly packed small hepatocytic cells, some of which were proliferative based on BrdU incorporation (Figure 5B). BrdU$^+$ cells were first detected in DEN-treated males and were confined to FAH and rarely detected in age-matched control mice. FAH contained cells positive for the same progenitor cell markers and activated signaling pathways present in HcPC-containing aggregates, including AFP, CD44, and EpCAM (Figure 5C). FAH also contained cells positive for activated STAT3, c-Jun, and PCNA (Figure 5C). Many cells within FAH exhibited strong upregulation of YAP (Figure 5C), a transcriptional coactivator that is negatively regulated by the Hippo pathway and a liver cancer oncoprotein (Zheng et al., 2011). FAH were also enriched in F4/80$^+$ macrophages (Figure 5C). These results suggest that the HcPC-containing aggregates may be derived from FAH.

HcPCs Exhibit Autocrine IL-6 Expression Necessary for HCC Progression

In situ hybridization (ISH) and immunohistochemistry (IHC) revealed that DEN-induced FAH contained IL-6-expressing cells (Figures 6A, 6B, and S5), and freshly isolated DEN-induced aggregates contained more IL-6 messenger RNA (mRNA) than nonaggregated hepatocytes (Figure 6C). We examined several

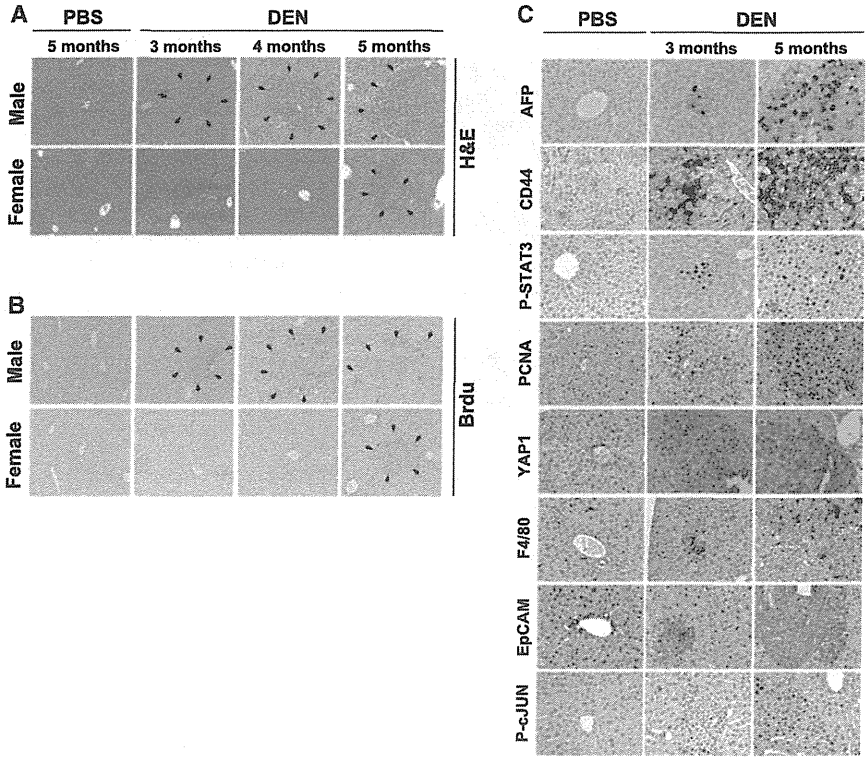

Figure 5. HcPC-Containing Aggregates May Originate from Liver Premalignant Lesions

(A and B) Male and female mice were injected with PBS or DEN at 15 days. At the indicated time points, BrdU was administrated, and livers were collected 2 hr later and stained with H&E (A) or a BrdU-specific antibody (B). Arrows indicate borders of FAH (magnification: 200×).

(C) Sections of male livers treated as above were subjected to IHC with the indicated antibodies (400×).

factors that control IL-6 expression and found that LIN28A and B were significantly upregulated in HcPCs and HCC (Figures 6D and 6E). LIN28-expressing cells were also detected within FAH (Figure 6F). As reported (Iliopoulos et al., 2009), knockdown of *LIN28B in cultured HcPC or HCC cell lines decreased* IL-6 expression (Figure 6G). LIN28 exerts its effects through downregulation of the microRNA (miRNA) Let-7 (Iliopoulos et al., 2009). Accordingly, miRNA array analysis of aggregated and nonaggregated hepatocytes from DEN-treated mice indicated that the amount of Let-7, along with other miRNAs that also inhibit IL-6 expression (miR194 and miR872), was lower in aggregated cells than in nonaggregated cells (Table S2).

To determine whether autocrine IL-6 production is needed for HCC growth, we silenced IL-6 expression with small hairpin RNA (shRNA) in dih10 HCC cells (He et al., 2010). This resulted in nearly a 75% decrease in IL-6 mRNA (Figure 7A) but had little effect on cell growth in the presence of growth factors, including EGF and insulin (Figure S6A). IL-6 mRNA silencing, however, diminished the ability of dih10 cells to form s.c. tumors (Figures S6B and S6C) and inhibited their ability to form HCCs and proliferate after transplantation into MUP-uPA mice (Figures 7B and S6D). To investigate the importance of autocrine IL-6 production at an earlier step, we isolated HcPC from DEN-treated WT and *Il6*$^{-/-}$ mice. Although IL-6 ablation attenuates HCC induction (Naugler et al., 2007), we still could isolate collagenase-resistant aggregates from livers of DEN-injected *Il6*$^{-/-}$ mice. Notably, IL-6 ablation did not reduce the proportion of CD44^{+} cells in the aggregates (Figures S7A and S7B). We introduced an identical number of WT and *Il6*$^{-/-}$ aggregated hepatocytes into MUP-uPA mice and scored HCC development 5 months later. The IL-6 deficiency resulted in a 2.5-fold decrease in tumorigenic potential (Figure 7C), suggesting that autocrine IL-6 contributes to HcPC to HCC progression. To confirm this point, we dispersed freshly isolated DEN-induced aggregates and transduced them with bicistronic lentiviruses encoding either scrambled or IL-6-specific shRNAs and a GFP marker. After a few days in culture, the transduced cells were introduced into MUP-uPA mice that were examined for HCC development 6 months later. Silencing of IL-6 reduced HCC generation (Figure 7D) and inhibited formation of GFP^{+} colonies within the MUP-uPA liver (Figure 7E). We also ablated IL-6 expression in mouse hepatocytes and found that this led to a marked reduction in DEN-induced tumorigenesis (Figure 7F). Thus, autocrine IL-6 production by DEN-initiated HcPC is important for HCC development. To investigate whether autocrine IL-6 signaling also occurs in human premalignant lesions, we examined needle biopsies of normal liver tissue and HCV-infected livers with dysplastic lesions. We found that 16% of all (n = 25) dysplastic lesions exhibited coexpression of LIN28 and IL-6 and contained activated STAT3 (Figure 7G). These markers were hardly detected in normal liver or nontumor portion of HCV-infected livers.

DISCUSSION

The isolation and characterization of cells that can give rise to HCC only after transplantation into an appropriate host liver undergoing chronic injury demonstrates that cancer arises from progenitor cells that are yet to become fully malignant. Importantly, unlike fully malignant HCC cells, the HcPCs we isolated cannot form s.c. tumors or even liver tumors when introduced into a nondamaged liver. Liver damage induced by uPA expression or CCl_4 treatment provides HcPCs with the proper cytokine and growth factor milieu needed for their proliferation. Although HcPCs produce IL-6, they may also depend on other cytokines such as TNF, which is produced by macrophages that are recruited to the damaged liver. In addition, uPA expression and CCl_4 treatment may enhance HcPC growth and progression through their fibrogenic effect on hepatic stellate cells. Although HCC and other cancers have been suspected to arise from

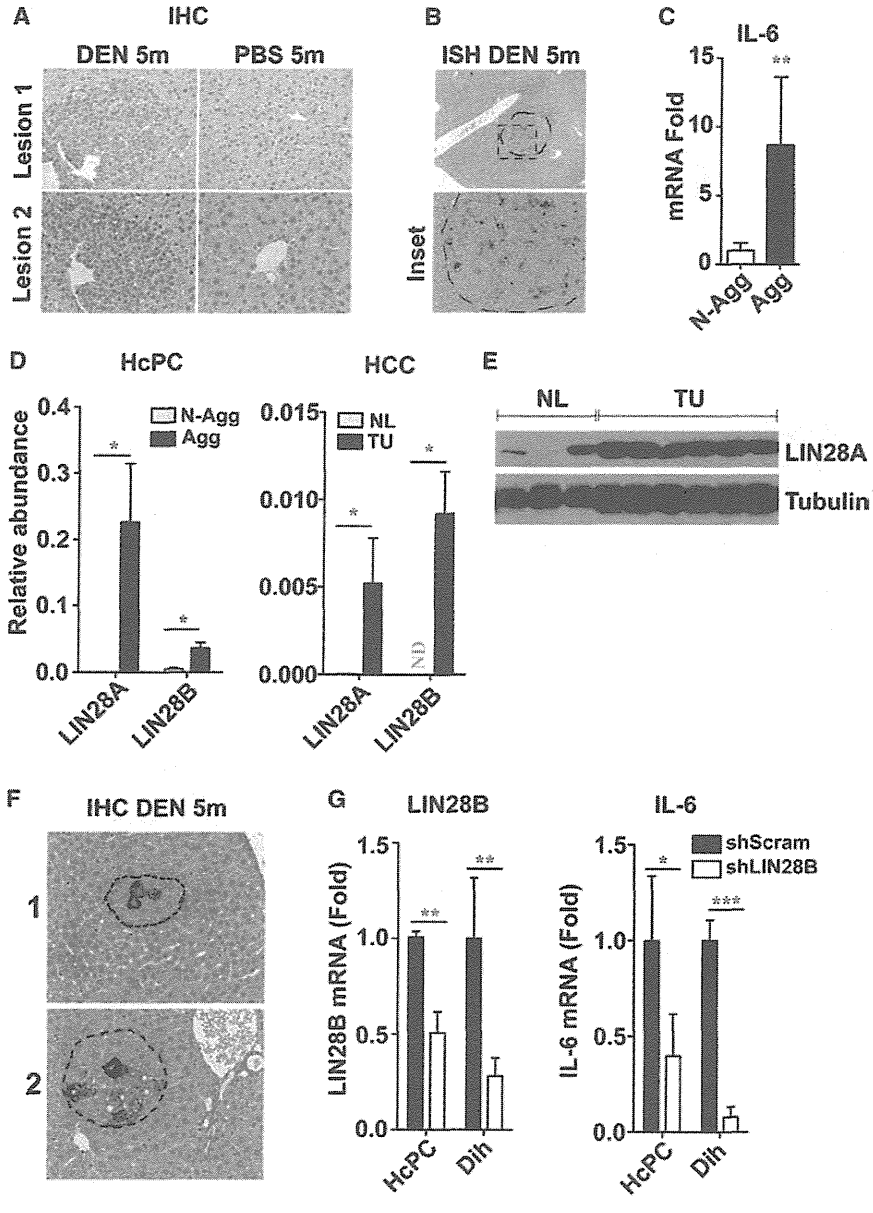

Figure 6. Liver Premalignant Lesions and HcPCs Exhibit Elevated IL-6 and LIN28 Expression

(A and B) Livers of 5-month-old DEN injected mice were analyzed for IL-6 expression by IHC (magnification: 400×) (A) and ISH (magnification: 100×, top; 400×, bottom) (B).

(C and D) Quantification of IL-6 (C) and LIN28 (D) mRNA in aggregated versus nonaggregated hepatocytes from 5-month-old DEN-treated livers and in normal versus tumor-bearing livers (n = 6; ± SEM) (ND, not detected).

(E) Immunoblot analyses of LIN28A in normal (NL) and tumor-bearing (TU) livers.

(F) DEN-treated livers were subjected to IHC with a LIN28A antibody. Broken lines indicate borders of FAH (400×).

(G) LIN28B was silenced with shRNA in HCC (dih) cells and cultured HcPCs, and LIN28B and IL-6 mRNAs were quantitated by qRT-PCR (n = 3; ± SEM).

See also Figure S5 and Table S2.

premalignant/dysplastic lesions (Hruban et al., 2007; Hytiroglou et al., 2007), a direct demonstration that such lesions progress into malignant tumors has been lacking. Based on expression of common markers—EpCAM, CD44, AFP, activated STAT3, and IL-6—that are not expressed in normal hepatocytes, we postulate that HcPCs originate from FAH or dysplastic foci, which are first observed in male mice within 3 months of DEN exposure. Indeed, the cells that are contained within the FAH are smaller than the surrounding parenchyma and are similar in size to isolated HcPCs. Importantly, FAH or premalignant dysplastic foci are not unique to DEN-treated rodents (Bannasch, 1984; Rabes, 1983), and similar lesions were detected in human cirrhotic livers (Hytiroglou et al., 2007; Seki et al., 2000; Takayama et al., 1990) in which the rate of HCC progression is 3%–5% per year (El-Serag, 2011). We found that human dysplastic lesions and mouse FAH and HcPC exhibit autocrine IL-6 signaling. HcPC are not unique to DEN-treated mice, and similar cells were isolated from *Tak1*$^{\Delta hep}$ mice in which HCC development resembles cirrhosis-associated human HCC (Inokuchi et al., 2010).

HcPC Origin and Relationship to Liver and HCC Stem Cells

Transcriptomic analysis indicates that DEN-induced HcPCs are related to both normal hepatobiliary bipotential stem cells/oval cells and HCC cells. Although HcPCs are not fully transformed, they express several markers—CD44, EpCAM, AFP, SOX9, OV6, and CK19—found to be expressed by HCC stem cells and oval cells (Guo et al., 2012; Mikhail and He, 2011; Terris et al., 2010; Yamashita et al., 2008; Zhu et al., 2010). However, unlike oval cells, which do not express albumin or AFP and do not give rise to liver tumors upon transplantation into MUP-uPA mice, HcPCs give rise to HCC after intrasplenic transplantation. Yet, unlike dih10 HCC cells, which express high levels of the HCC stem cell markers AFP, CD44, and EpCAM, HcPCs do not form s.c. tumors.

At this point, it is not clear whether HcPCs arise from oval cells or from dedifferentiated hepatocytes. Given that DEN is metabolically activated by Cyp2E1 that is expressed only in fully differentiated zone 3 hepatocytes (Tsutsumi et al., 1989) and that *Cyp2E1*$^{-/-}$ mice are refractory to DEN (Kang et al., 2007), DEN-induced HcPC are most likely derived from dedifferentiated hepatocytes. Consistent with this hypothesis, DEN-induced FAH and proliferating cells were found in zone 3 and not near bile ducts or the canals of Hering, sites at which oval cells reside

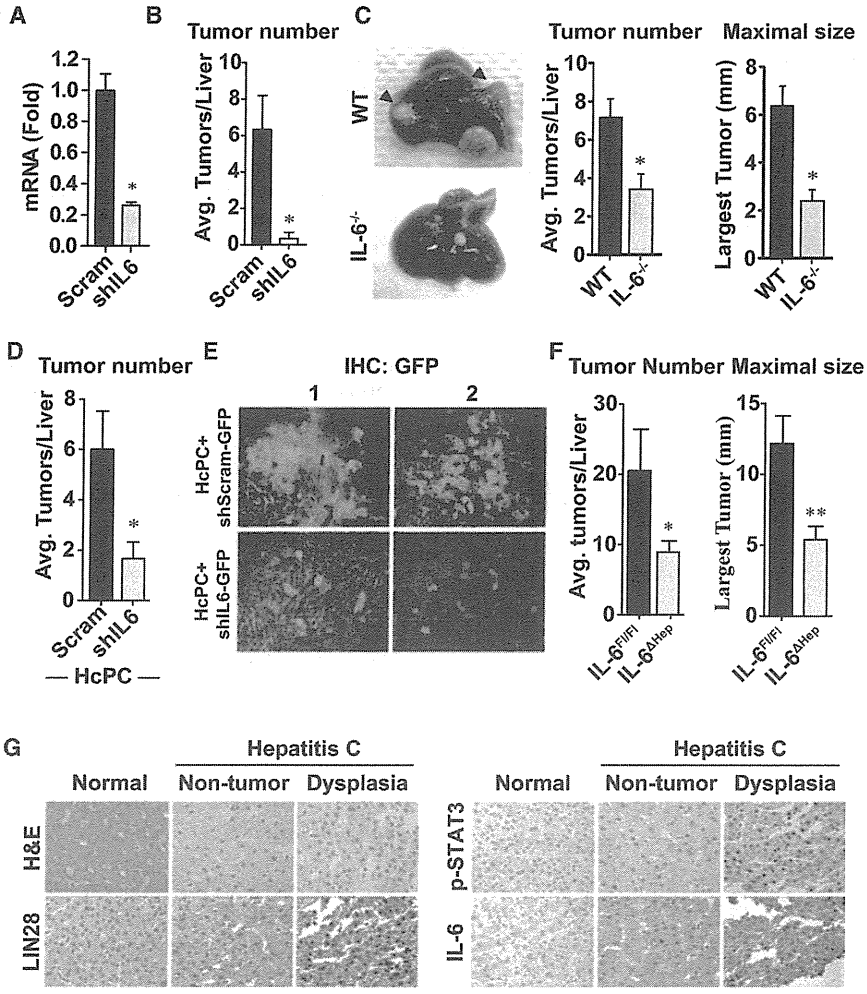

Figure 7. HCC Growth Depends on Autocrine IL-6 Production

(A) HCC cells (dih10) were transduced with lentiviruses containing scrambled or IL-6-specific shRNA. IL-6 mRNA was analyzed by qRT-PCR.

(B) Dih10 cells (1.2×10^5) transduced as above were i.s. injected into MUP-uPA mice that were analyzed 6 months later for HCC development (n = 3; ± SEM).

(C) HcPCs from WT and *Il6*$^{-/-}$ mice were injected (1×10^4 cells/mice) into MUP-uPA mice and analyzed 5 months later for HCC development (n = 5; ± SEM).

(D) HcPCs isolated from DEN-treated WT mice were transduced with shRNA against IL-6 or scrambled shRNA, cultured for 3 to 4 days, i.s. transplanted (1×10^4 cells/mice) into MUP-uPA mice, and analyzed 6 months later (n = 3; ± SEM).

(E) Livers of MUP-uPA mice from (D) were immunostained with GFP antibody 6 months after transplantation (200×). The bicistronic lentivirus in this experiment expresses GFP along with control or IL-6 shRNA, allowing tracking of the infected cells.

(F) DEN-treated *Il6*$^{\Delta hep}$ and *Il6*$^{F/F}$ mice were sacrificed after 9 months to evaluate tumor multiplicity and size (n = 6–10, ± SEM).

(G) IHC analysis of autocrine IL-6 signaling in human premalignant lesions in HCV-infected livers. Expression of LIN28, p-STAT3, and IL-6 was analyzed in 25 needle biopsies of dysplastic nodules, and representative positive specimens (n = 4) are shown. The dysplastic nodules and paired nontumor tissue were obtained from the same HCV-infected patient (n = 25). Nontumor tissue of metastatic liver cancer was used as normal control.

See also Figures S6 and S7.

(Duncan et al., 2009). Notably, GO analysis revealed that many of the genes whose expression is downregulated in HcPC-containing aggregates are involved in xenobiotic and organic acid metabolism, characteristics of differentiated hepatocytes. The same types of genes are also downregulated in HCC. However, final identification of the origin of HcPC will be provided by ongoing lineage-tracing experiments.

The Significance of Autocrine IL-6 Expression

Elevated IL-6 was detected in at least 40% of human HCCs, where it is expressed by the cancer cells (Soresi et al., 2006). More recent studies have confirmed upregulation of IL-6 in human HCC and suggested that it plays a central role in a gene expression network that drives tumor development (Ji et al., 2009). Elevated IL-6 was also found in viral and alcoholic hepatitis and liver cirrhosis, but in these conditions, IL-6 is expressed mainly by myeloid cells/leukocytes rather than parenchymal cells (Deviere et al., 1989; Kakumu et al., 1993; Soresi et al., 2006). Our studies indicate that the critical site of IL-6 expression shifts from myeloid cells to epithelial cells during the course of DEN-induced liver tumorigenesis. Initially, DEN administration rapidly induces IL-6 in Kupffer cells through NF-κB activation (Maeda et al., 2005). This initial surge in IL-6 is required for DEN-induced hepatocarcinogenesis (Naugler et al., 2007). Although IL-6 decays within 2 weeks of DEN administration, it reappears several months later, but at that time, it is expressed within FAH. IL-6 expression is also elevated in isolated HcPCs and is maintained in fully transformed HCC cells. Furthermore, autocrine IL-6 is important for HcPC to HCC progression and for tumorigenic growth. Autocrine IL-6 in both HcPC and HCC cells depends on elevated expression of LIN28, an RNA-binding protein that exerts its protumorigenic activity through downregulation of Let-7, an miRNA that inhibits IL-6 expression (Viswanathan and Daley, 2010). Accordingly, HcPCs exhibit downregulation of both Let-7f and Let-7g, and elevated LIN28 is found not only in isolated HcPCs but also within FAH and human HCV-induced dysplastic lesions.

A similar LIN28-Let-7-IL-6 epigenetic switch is important for in vitro programming and maintenance of cancer stem cells (Iliopoulos et al., 2009). IL-6 also induces malignant features in human ductal carcinoma stem cells (Sansone et al., 2007). In fact, autocrine IL-6 signaling was suggested to play a key role in STAT3-dependent tumor progression (Grivennikov and Karin, 2008). Another miRNA-driven autoregulatory circuit involved in

hepatocarcinogenesis accounts for elevated IL-6R expression (Hatziapostolou et al., 2011). Yet, HcPC-containing aggregates also express several other STAT3-activiting cytokines and receptors. Accordingly, silencing or ablation of IL-6 results in incomplete inhibition of HcPC to HCC progression. Nonetheless, our results demonstrate that autoregulatory circuits/epigenetic switches play an important role in the very early stages of tumorigenesis. Given that such circuits are already activated in premalignant cells, pharmacological agents that disrupt their function may be useful in cancer prevention. Prevention is of particular importance in cancers such as HCC, which is often detected at a stage that is refractory to currently available therapeutics.

EXPERIMENTAL PROCEDURES

Mice, HCC Induction, HcPC Isolation, and Transplantation

MUP-uPA transgenic mice (Weglarz et al., 2000) were maintained on a pure BL/6 background. Because homozygous females frequently die when pregnant, MUP-uPA heterozygotes were generated by backcrossing homozygous MUP-uPA males with BL/6 females to be used as recipients for hepatic transplantation. *Tak1*$^{\Delta hep}$ (Inokuchi et al., 2010) and *Il6*$^{F/F}$ (Quintana et al., 2013) mice were also in the BL/6 background. *Il6*$^{\Delta hep}$ mice were generated by crossing *Il6*$^{F/F}$ and *Alb-Cre* mice. C57BL/6 actin-GFP mice were from the Jackson Laboratories. BL/6 mice were purchased from Charles River Laboratories.

To induce HCC, 15-day-old mice were injected i.p. with 25 mg/kg DEN (Sigma). A pool of DEN-injected BL/6 mice was maintained and used in most experiments. Hepatocytes were isolated using a two-step procedure (He et al., 2010). Cell aggregates were isolated by filtration through 70 and 40 μm sieves. To disperse the aggregates into single cells, they were subjected to gentle pipetting in Ca/Mg-free PBS on ice. Single-cell suspensions of aggregated and nonaggregated hepatocytes were transplanted via an i.s. injection into 21-day-old male MUP-uPA mice (He et al., 2010). Alternatively, single-cell suspensions of aggregated hepatocytes were enriched for CD44^{+} HcPC using magnetic beads. As few as 100 viable CD44^{+} cells mixed with 1 × 10^{5} normal hepatocytes from normal males were transplanted into MUP-uPA mice. Alternatively, BL/6 mice were pretreated with retrorsine (70 mg/kg i.p.) (Sigma), a cell-cycle inhibitor, 1 month prior to transplantation. Transplanted mice were allowed to recover for 1 week and then injected weekly with 3× 0.5 ml/kg CCl_4 i.p. to induce liver injury and hepatocyte proliferation (Guo et al., 2002). Mice were sacrificed 5 to 6 months later, and tumors bigger than 1 mm in diameter on the liver surface were counted. Tumors bigger than 5 mm across were dissected for biochemical and molecular analyses.

ACCESSION NUMBERS

Raw gene expression array data have been deposited to NCBI's Gene Expression Omnibus under the GSE50431 study.

SUPPLEMENTAL INFORMATION

Supplemental Information includes Extended Experimental Procedures, seven figures, and three tables and can be found with this article online at http://dx.doi.org/10.1016/j.cell.2013.09.031.

AUTHOR CONTRIBUTIONS

G.H. identified, isolated, and characterized HcPCs; D.D. and H.N. optimized the HcPC isolation and purification procedure; D.D. found the mechanism of their dependence on autocrine IL-6 controlled by LIN28, characterized them using flow cytometry (with S.S.), and conducted miR analyses (with M.H. and D.I.); H.N. and D.D. used *Il6*$^{\Delta hep}$ mice to demonstrate in vivo HCC dependency on autocrine IL-6; H.N. (with R.T. and K.K.) found IL-6, LIN28, and P-STAT3 in human dysplastic lesions; J.F.-B. conducted the transcriptome analysis and exome sequencing (with S.E.Y., K.J., and O.H.) and with H.O. examined oncogenic potential of oval cells; H.O. examined HcPC proliferative potential and performed IF analysis of isolated HcPC (with A.S. and R.M.H.); Y.J. assisted with IHC and ISH staining; E.S. contributed to the experiments involving *Tak1*$^{\Delta hep}$ mice; G.H., D.D., J.F.-B., H.O., and M.K. wrote the manuscript.

ACKNOWLEDGMENTS

We acknowledge the Biogem facility at UCSD for their assistance with transcriptome analysis and A. Arian, K. Iwaisako, Y. Hiroshima, and H. Matsui for technical assistance. We thank Dr. J. Hidalgo (Universitat Autonoma de Barcelona, Spain) for the *Il6*$^{F/F}$ mice. Research was supported by the Superfund Basic Research Program (P42ES010337), NIH (CA118165 and CA155120), Wellcome Trust (WT086755), American Diabetes Association (7-08-MN-29), the Center for Translational Science (UL1RR031980 and UL1TR000100), the National Center for Research Resources IMAT program (N12R1CA155615), and postdoctoral research fellowships from the Damon Runyon Cancer Research Foundation (G.H.), American Liver Foundation (D.D.), Daiichi Sankyo Foundation of Life Science (H.N.), California Institute for Regenerative Medicine Stem Cell Training Grant II (TG2-01154) fellowship (J.F.-B.), Kanzawa Medical Research Foundation (H.O.), the German Research Foundation (DFG, SH721/1-1 to S.S.), and a Young Investigator Award from the National Childhood Cancer Foundation, "CureSearch" (D.D.). M.K. is an ACS Research Professor and is a recipient of the Ben and Wanda Hildyard Chair for Mitochondrial and Metabolic Diseases.

Received: December 11, 2012
Revised: June 4, 2013
Accepted: September 19, 2013
Published: October 10, 2013

REFERENCES

Bannasch, P. (1984). Sequential cellular changes during chemical carcinogenesis. J. Cancer Res. Clin. Oncol. *108*, 11–22.

Bladt, F., Riethmacher, D., Isenmann, S., Aguzzi, A., and Birchmeier, C. (1995). Essential role for the c-met receptor in the migration of myogenic precursor cells into the limb bud. Nature *376*, 768–771.

Deviere, J., Content, J., Denys, C., Vandenbussche, P., Schandene, L., Wybran, J., and Dupont, E. (1989). High interleukin-6 serum levels and increased production by leucocytes in alcoholic liver cirrhosis. Correlation with IgA serum levels and lymphokines production. Clin. Exp. Immunol. *77*, 221–225.

Dorrell, C., Erker, L., Schug, J., Kopp, J.L., Canaday, P.S., Fox, A.J., Smirnova, O., Duncan, A.W., Finegold, M.J., Sander, M., et al. (2011). Prospective isolation of a bipotential clonogenic liver progenitor cell in adult mice. Genes Dev. *25*, 1193–1203.

Duncan, A.W., Dorrell, C., and Grompe, M. (2009). Stem cells and liver regeneration. Gastroenterology *137*, 466–481.

Eferl, R., Ricci, R., Kenner, L., Zenz, R., David, J.P., Rath, M., and Wagner, E.F. (2003). Liver tumor development. c-Jun antagonizes the proapoptotic activity of p53. Cell *112*, 181–192.

El-Serag, H.B. (2011). Hepatocellular carcinoma. N. Engl. J. Med. *365*, 1118–1127.

Grivennikov, S., and Karin, M. (2008). Autocrine IL-6 signaling: a key event in tumorigenesis? Cancer Cell *13*, 7–9.

Guichard, C., Amaddeo, G., Imbeaud, S., Ladeiro, Y., Pelletier, L., Maad, I.B., Calderaro, J., Bioulac-Sage, P., Letexier, M., Degos, F., et al. (2012). Integrated analysis of somatic mutations and focal copy-number changes identifies key genes and pathways in hepatocellular carcinoma. Nat. Genet. *44*, 694–698.

Guo, D., Fu, T., Nelson, J.A., Superina, R.A., and Soriano, H.E. (2002). Liver repopulation after cell transplantation in mice treated with retrorsine and carbon tetrachloride. Transplantation *73*, 1818–1824.

Guo, X., Xiong, L., Sun, T., Peng, R., Zou, L., Zhu, H., Zhang, J., Li, H., and Zhao, J. (2012). Expression features of SOX9 associate with tumor progression and poor prognosis of hepatocellular carcinoma. Diagn. Pathol. *7*, 44.

Haridass, D., Yuan, Q., Becker, P.D., Cantz, T., Iken, M., Rothe, M., Narain, N., Bock, M., Nörder, M., Legrand, N., et al. (2009). Repopulation efficiencies of adult hepatocytes, fetal liver progenitor cells, and embryonic stem cell-derived hepatic cells in albumin-promoter-enhancer urokinase-type plasminogen activator mice. Am. J. Pathol. *175*, 1483–1492.

Hatziapostolou, M., Polytarchou, C., Aggelidou, E., Drakaki, A., Poultsides, G.A., Jaeger, S.A., Ogata, H., Karin, M., Struhl, K., Hadzopoulou-Cladaras, M., and Iliopoulos, D. (2011). An HNF4α-miRNA inflammatory feedback circuit regulates hepatocellular oncogenesis. Cell *147*, 1233–1247.

He, G., Yu, G.Y., Temkin, V., Ogata, H., Kuntzen, C., Sakurai, T., Sieghart, W., Peck-Radosavljevic, M., Leffert, H.L., and Karin, M. (2010). Hepatocyte IKKbeta/NF-kappaB inhibits tumor promotion and progression by preventing oxidative stress-driven STAT3 activation. Cancer Cell *17*, 286–297.

Hruban, R.H., Maitra, A., Kern, S.E., and Goggins, M. (2007). Precursors to pancreatic cancer. Gastroenterol. Clin. North Am. *36*, 831–849, vi.

Hytiroglou, P., Park, Y.N., Krinsky, G., and Theise, N.D. (2007). Hepatic precancerous lesions and small hepatocellular carcinoma. Gastroenterol. Clin. North Am. *36*, 867–887, vii.

Ichinohe, N., Kon, J., Sasaki, K., Nakamura, Y., Ooe, H., Tanimizu, N., and Mitaka, T. (2012). Growth ability and repopulation efficiency of transplanted hepatic stem cells, progenitor cells, and mature hepatocytes in retrorsine-treated rat livers. Cell Transplant. *21*, 11–22.

Iliopoulos, D., Hirsch, H.A., and Struhl, K. (2009). An epigenetic switch involving NF-kappaB, Lin28, Let-7 MicroRNA, and IL6 links inflammation to cell transformation. Cell *139*, 693–706.

Inokuchi, S., Aoyama, T., Miura, K., Osterreicher, C.H., Kodama, Y., Miyai, K., Akira, S., Brenner, D.A., and Seki, E. (2010). Disruption of TAK1 in hepatocytes causes hepatic injury, inflammation, fibrosis, and carcinogenesis. Proc. Natl. Acad. Sci. USA *107*, 844–849.

Ji, J., Shi, J., Budhu, A., Yu, Z., Forgues, M., Roessler, S., Ambs, S., Chen, Y., Meltzer, P.S., Croce, C.M., et al. (2009). MicroRNA expression, survival, and response to interferon in liver cancer. N. Engl. J. Med. *361*, 1437–1447.

Kakumu, S., Shinagawa, T., Ishikawa, T., Yoshioka, K., Wakita, T., and Ida, N. (1993). Interleukin 6 production by peripheral blood mononuclear cells in patients with chronic hepatitis B virus infection and primary biliary cirrhosis. Gastroenterol. Jpn. *28*, 18–24.

Kang, J.S., Wanibuchi, H., Morimura, K., Gonzalez, F.J., and Fukushima, S. (2007). Role of CYP2E1 in diethylnitrosamine-induced hepatocarcinogenesis in vivo. Cancer Res. *67*, 11141–11146.

Laconi, E., Oren, R., Mukhopadhyay, D.K., Hurston, E., Laconi, S., Pani, P., Dabeva, M.D., and Shafritz, D.A. (1998). Long-term, near-total liver replacement by transplantation of isolated hepatocytes in rats treated with retrorsine. Am. J. Pathol. *153*, 319–329.

Maeda, S., Kamata, H., Luo, J.L., Leffert, H., and Karin, M. (2005). IKKbeta couples hepatocyte death to cytokine-driven compensatory proliferation that promotes chemical hepatocarcinogenesis. Cell *121*, 977–990.

Marquardt, J.U., and Thorgeirsson, S.S. (2010). Stem cells in hepatocarcinogenesis: evidence from genomic data. Semin. Liver Dis. *30*, 26–34.

Meyer, K., Lee, J.S., Dyck, P.A., Cao, W.Q., Rao, M.S., Thorgeirsson, S.S., and Reddy, J.K. (2003). Molecular profiling of hepatocellular carcinomas developing spontaneously in acyl-CoA oxidase deficient mice: comparison with liver tumors induced in wild-type mice by a peroxisome proliferator and a genotoxic carcinogen. Carcinogenesis *24*, 975–984.

Mikhail, S., and He, A.R. (2011). Liver cancer stem cells. Int. J. Hepatol. *2011*, 486954.

Naugler, W.E., Sakurai, T., Kim, S., Maeda, S., Kim, K., Elsharkawy, A.M., and Karin, M. (2007). Gender disparity in liver cancer due to sex differences in MyD88-dependent IL-6 production. Science *317*, 121–124.

Nguyen, L.V., Vanner, R., Dirks, P., and Eaves, C.J. (2012). Cancer stem cells: an evolving concept. Nat. Rev. Cancer *12*, 133–143.

Nowell, P.C. (1976). The clonal evolution of tumor cell populations. Science *194*, 23–28.

Park, E.J., Lee, J.H., Yu, G.Y., He, G., Ali, S.R., Holzer, R.G., Osterreicher, C.H., Takahashi, H., and Karin, M. (2010). Dietary and genetic obesity promote liver inflammation and tumorigenesis by enhancing IL-6 and TNF expression. Cell *140*, 197–208.

Pitot, H.C. (1990). Altered hepatic foci: their role in murine hepatocarcinogenesis. Annu. Rev. Pharmacol. Toxicol. *30*, 465–500.

Porta, C., De Amici, M., Quaglini, S., Paglino, C., Tagliani, F., Boncimino, A., Moratti, R., and Corazza, G.R. (2008). Circulating interleukin-6 as a tumor marker for hepatocellular carcinoma. Ann. Oncol. *19*, 353–358.

Quintana, A., Erta, M., Ferrer, B., Comes, G., Giralt, M., and Hidalgo, J. (2013). Astrocyte-specific deficiency of interleukin-6 and its receptor reveal specific roles in survival, body weight and behavior. Brain Behav. Immun. *27*, 162–173.

Rabes, H.M. (1983). Development and growth of early preneoplastic lesions induced in the liver by chemical carcinogens. J. Cancer Res. Clin. Oncol. *106*, 85–92.

Rhim, J.A., Sandgren, E.P., Degen, J.L., Palmiter, R.D., and Brinster, R.L. (1994). Replacement of diseased mouse liver by hepatic cell transplantation. Science *263*, 1149–1152.

Sansone, P., Storci, G., Tavolari, S., Guarnieri, T., Giovannini, C., Taffurelli, M., Ceccarelli, C., Santini, D., Paterini, P., Marcu, K.B., et al. (2007). IL-6 triggers malignant features in mammospheres from human ductal breast carcinoma and normal mammary gland. J. Clin. Invest. *117*, 3988–4002.

Seki, S., Sakaguchi, H., Kitada, T., Tamori, A., Takeda, T., Kawada, N., Habu, D., Nakatani, K., Nishiguchi, S., and Shiomi, S. (2000). Outcomes of dysplastic nodules in human cirrhotic liver: a clinicopathological study. Clin. Cancer Res. *6*, 3469–3473.

Sell, S., and Leffert, H.L. (2008). Liver cancer stem cells. J. Clin. Oncol. *26*, 2800–2805.

Shin, S., Walton, G., Aoki, R., Brondell, K., Schug, J., Fox, A., Smirnova, O., Dorrell, C., Erker, L., Chu, A.S., et al. (2011). Foxl1-Cre-marked adult hepatic progenitors have clonogenic and bilineage differentiation potential. Genes Dev. *25*, 1185–1192.

Soresi, M., Giannitrapani, L., D'Antona, F., Florena, A.M., La Spada, E., Terranova, A., Cervello, M., D'Alessandro, N., and Montalto, G. (2006). Interleukin-6 and its soluble receptor in patients with liver cirrhosis and hepatocellular carcinoma. World J. Gastroenterol. *12*, 2563–2568.

Su, Y., Kanamoto, R., Miller, D.A., Ogawa, H., and Pitot, H.C. (1990). Regulation of the expression of the serine dehydratase gene in the kidney and liver of the rat. Biochem. Biophys. Res. Commun. *170*, 892–899.

Su, Q., Benner, A., Hofmann, W.J., Otto, G., Pichlmayr, R., and Bannasch, P. (1997). Human hepatic preneoplasia: phenotypes and proliferation kinetics of foci and nodules of altered hepatocytes and their relationship to liver cell dysplasia. Virchows Arch. *431*, 391–406.

Takayama, T., Makuuchi, M., Hirohashi, S., Sakamoto, M., Okazaki, N., Takayasu, K., Kosuge, T., Motoo, Y., Yamazaki, S., and Hasegawa, H. (1990). Malignant transformation of adenomatous hyperplasia to hepatocellular carcinoma. Lancet *336*, 1150–1153.

Terris, B., Cavard, C., and Perret, C. (2010). EpCAM, a new marker for cancer stem cells in hepatocellular carcinoma. J. Hepatol. *52*, 280–281.

Tsutsumi, M., Lasker, J.M., Shimizu, M., Rosman, A.S., and Lieber, C.S. (1989). The intralobular distribution of ethanol-inducible P450IIE1 in rat and human liver. Hepatology *10*, 437–446.

Verna, L., Whysner, J., and Williams, G.M. (1996). N-nitrosodiethylamine mechanistic data and risk assessment: bioactivation, DNA-adduct formation, mutagenicity, and tumor initiation. Pharmacol. Ther. *71*, 57–81.

Viswanathan, S.R., and Daley, G.Q. (2010). Lin28: A microRNA regulator with a macro role. Cell *140*, 445–449.

Wang, R., Ferrell, L.D., Faouzi, S., Maher, J.J., and Bishop, J.M. (2001). Activation of the Met receptor by cell attachment induces and sustains hepatocellular carcinomas in transgenic mice. J. Cell Biol. *153*, 1023–1034.